ioMosaic®

Minimizing risk. Maximizing potential.®

Forget the Omega Method

Master ∫vdP Integration Instead

An ioMosaic White Paper

G. A. Melhem, Ph.D., FAIChE

melhem@iomosaic.com

This page intentionally left blank

IOMOSAIC CORPORATION

Forget the Omega Method and Master $\int vdP$ Integration Instead

Process Safety and Risk Management Practices

authored by

Georges A. MELHEM, Ph.D., FAIChE

January 12, 2023

Notice:

This document was prepared by ioMosaic Corporation (**ioMosaic**) for public release. This document represents ioMosaic's best judgment in light of information available and researched prior to the time of publication.

Opinions in this document are based in part upon data and information available in the open literature, data developed or measured by ioMosaic, and/or information obtained from ioMosaic's advisors and affiliates. The reader is advised that ioMosaic has not independently verified all the data or the information contained therein. This document must be read in its entirety. The reader understands that no assurances can be made that all liabilities have been identified. This document does not constitute a legal opinion.

No person has been authorized by ioMosaic to provide any information or make any representation not contained in this document. Any use the reader makes of this document, or any reliance upon or decisions to be made based upon this document are the responsibility of the reader. ioMosaic does not accept any responsibility for damages, if any, suffered by the reader based upon this document.

Contents

1 Introduction

Reliable flow estimates are essential for the sizing and selection of process equipment including but not limited to relief devices, process piping, and depressuring systems. In addition, reliable flow estimates from loss of containment scenarios can significantly influence the quality of consequence, risk analysis, and facility siting studies as well.

Existing methods for the calculation of flow rates range from those for simple, non-reacting, single phase, steady state flow to methods for dynamic, multiphase, reacting flows. Ideal nozzle flow calculation methods are heavily used in relief systems and risk analysis studies and are detailed in numerous standards and industry guidelines including the International Organization for Standardization (ISO), the American Society of Mechanical Engineers (ASME), the American Institute of Chemical Engineers (AIChE) Center for Chemical Process Safety (CCPS) and Design Institute for Emergency Relief Systems (DIERS), and the American Petroleum Institute (API).

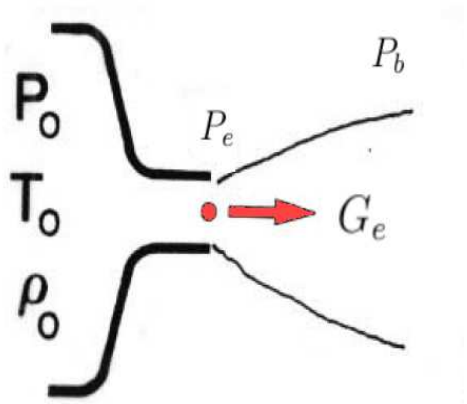

Relief systems studies often include different types of flows such as non-equilibrium, subcooled, liquid, vapor, twophase, supercritical, and retrograde and phase change (RPC) flows [1, 2]. Flow estimates can be influenced by vapor quality, the presence of solids, slip, viscosity, chemical reactions, piping and fittings losses and geometry, chemical composition, temperature, pressure, etc. In addition to flow rates, reliable flow methods are expected to yield reliable estimates for reaction forces, location of choke points, sound power levels, exit temperatures and pressures, exit compositions and vapor quality, twophase flow regimes, etc.

We explore in this document the origins of ideal nozzle flow methods for single and multiphase flow including Δh, direct vdP integration ($\int vdP$), simple reduced analytical models, and complex reduced analytical models. We also explore the advantages and disadvantages of those methods for simple and complex flow systems.

2 The Thermodynamics of Nozzle Flow

The origin of all ideal nozzle flow methods can be traced back to the first law of thermodynamics or conservation of energy. Let's consider a vessel containing a multiphase mixture that is exchanging mass and energy with its surroundings. If we define our thermodynamic system to include all the vessel contents, we can write the first law of thermodynamics as follows:

$$\frac{d}{dt}(me) = \dot{m}_{in}\left(h_{in} + \frac{u_{in}^2}{2} + gz_{in}\right) - \dot{m}_{out}\left(h_{out} + \frac{u_{out}^2}{2} + gz_{out}\right) + \frac{dq}{dt} - \frac{dw}{dt} \quad (1)$$

where t is time, e is the specific internal energy of the vessel contents, h is the specific enthalpy, m is vessel contents mass, $\dot{m}$ is the mass flow rate, z is elevation, g is the gravitational constant, q is the heating rate gained by the vessel contents from the surroundings, and w is the work performed by the vessel contents on the surroundings.

At steady state, we can also express Equation 1 in differential form:

$$dh + gdz + udu = dq - dw \tag{2}$$

If we ignore elevation changes and energy exchange with the surroundings, Equation 2 becomes:

$$dh + udu = 0 \text{ or } \int_{h_o}^{h_e} dh + \int_{u_o}^{u_e} udu = 0 \text{ or } u_e = \sqrt{2\left(h_o - h_e\right) + u_o^2} \tag{3}$$

where $_o$ represents inlet conditions, and $_e$ represents exit conditions. Equation 3 is the primary source of all nozzle flow equations. It is often expressed in a form that yields the flow exit velocity, u_e or mass flux, G_e:

$$u_e = \sqrt{2\Delta h + u_o^2} \text{ or } G_e = \rho_e\sqrt{2\Delta h + u_o^2} \text{ where } \Delta h = h_o - h_e \tag{4}$$

We note that Equation 4 includes the entrance velocity to the thermodynamic system. For a vessel, u_o is normally set to 0. However, performing a nozzle calculation for a nozzle located downstream from a vessel will require the approach or inlet velocity u_o or the use of stagnation specific enthalpy $h_o + \frac{1}{2}u_o^2$.

In order for Equation 4 to yield the mass flow rate and exit conditions, a thermodynamic path needs to be selected first. Then the exit pressure needs to be selected such that the calculated mass flux, G_e is maximized. Normally, an isentropic (constant entropy) thermodynamic path is selected. The specific enthalpy values require the use of an equation of state. The specific enthalpy used in Equation 4 can be expressed to include multiphase mixtures.

3 Generalized Nozzle Flow Solutions

Generalized nozzle flow solvers calculate the mass flux and exit conditions using the following steps:

1. Calculate h_o at T_o and P_o using an equation of state. If the starting conditions include multiple phases, then h_o is calculated based on the contributions of each phase.
2. Select a pressure step, ΔP
3. Set P_e to $P_o - \Delta P$. P_e will be bounded between the surroundings pressure or backpressure, P_b and the starting pressure, P_o.
4. Calculate the exit temperature T_e and the phase split at the exit conditions T_e and P_e such that the thermodynamic constraint or path is satisfied, normally isentropic, or $\Delta s = s_o - s_e = 0$.

5. Calculate the mass flux G_e from Equation 4.

6. If the maximum value of G_e is not reached, i.e. G_e is still increasing, go back to step 3. If P_e is equal to P_b, then the flow is subsonic, stop. If G_e is less then the value calculated in the previous step, decrease the pressure step size until a certain pressure tolerance is achieved. Once ΔP is small enough, P_e is reached and is the choke point or the pressure at which sonic flow is achieved.

Equation 4 is suitable for all types of flow including flashing flows and RPC flows. However, high accuracy estimates of specific enthalpies and phase splits are required. These accuracies cannot be achieved without accurate numerical evaluations, i.e. table lookups for enthalpies and vapor quality may not work well for multiphase flow estimates.

Equation 4 is usually expressed in terms of mass flow rate by multiplying the mass flux G_e by a nozzle flow area, A_e.

$$\frac{dm_{out}}{dt} = \dot{m}_{out} = A_e G_e \tag{5}$$

The flow through a well rounded converging nozzle can approach that of an ideal nozzle where irrecoverable pressure losses are negligible. A converging nozzle can produce substantial kinetic energy, especially for high velocity gas flow. Even well rounded nozzles are not perfectly ideal. As a result, the mass flux G_e is also multiplied by a flow discharge coefficient, C_d, to account for the thermodynamic efficiency reduction of the nozzle.

$$\frac{dm_{out}}{dt} = \dot{m}_{out} = A_e G_e C_d \tag{6}$$

4 Nozzle Flow Thermodynamic Efficiency

The use of a discharge coefficient for a converging nozzle flow is a representation of the thermodynamic efficiency of the nozzle:

$$\eta_{c,s} = \frac{h_o - h_e}{h_o - h_{e,s}} \tag{7}$$

$$C_d = \frac{G_e}{G_{e,s}} = \frac{\rho_e u_e}{\rho_{e,s} u_{e,s}} = \frac{\rho_e}{\rho_{e,s}} \frac{\sqrt{2\eta_c \left(h_o - h_{e,s}\right)}}{\sqrt{2\left(h_o - h_{e,s}\right)}} \tag{8}$$

$$C_d = \frac{\rho_e}{\rho_{e,s}} \sqrt{\eta_{c,s}} \simeq \sqrt{\eta_{c,s}} \text{ or } \eta_{c,s} \simeq C_d^2 \simeq \frac{u_e^2}{u_{e,s}^2} \tag{9}$$

where $\eta_{c,s}$ is the thermodynamic efficiency or isentropic efficiency. A nozzle with a discharge coefficient of 0.975 is equivalent to a nozzle with approximately 95 % thermodynamic efficiency.

For a diverging nozzle, the thermodynamic efficiency is calculated similarly and the final exit state will have a positive entropy change such that:

$$h_o - h_e = \eta_{d,s}\left(h_o - h_{e,s}\right) \tag{10}$$

$$\eta_{d,s} = \frac{h_o - h_e}{h_o - h_{e,s}} \tag{11}$$

where h_o is the specific enthalpy of the fluid at the inlet of the diverging nozzle and h_e is the specific enthalpy at the exit of the diverging nozzle.

5 Ideal Gas Nozzle Flow

Even with high speed computing and the availability of several useful and accurate equations of state, many engineers still rely on a constant γ ideal gas equation of state for fluid flow. This is used for example when calculating the hydraulics of flare headers at low pressure and one dimensional gas flow dynamics. A constant value of γ is used to define the equation of state and all the associated thermodynamic properties:

$$\gamma = \frac{C_p}{C_v} = \frac{C_p}{C_p - R_g} \text{ or } C_p = R_g\frac{\gamma}{\gamma - 1} \tag{12}$$

where R_g is ideal gas constant, C_p is the molar ideal gas heat capacity at constant pressure, C_v is the molar ideal gas heat capacity at constant volume, and γ is the ideal gas heat capacity ratio. For an ideal gas, the pressure, specific enthalpy, and specific internal energy can be calculated using the following expressions:

$$P = \rho e\left(\gamma - 1\right) = \frac{\rho R_g T}{M_w} \tag{13}$$

$$e = \frac{P}{\rho\left(\gamma - 1\right)} = \frac{R_g T}{M_w\left(\gamma - 1\right)} = \frac{c_s^2}{\gamma\left(\gamma - 1\right)} \tag{14}$$

$$h = e + \frac{P}{\rho} = \frac{P}{\rho}\left(\frac{\gamma}{\gamma - 1}\right) = \frac{R_g T}{M_w}\left(\frac{\gamma}{\gamma - 1}\right) = \frac{c_s^2}{\left(\gamma - 1\right)} \tag{15}$$

where P is the static pressure, T is the static temperature, and M_w is the average molecular weight. It can be shown that the speed of sound under isentropic conditions, c_s, is equal to:

$$c_s^2 = \frac{\gamma R_g T}{M_w} = \left[\frac{\partial P}{\partial \rho}\right]_s = \frac{1}{\rho \kappa_s} \text{ where } \kappa_s = \frac{1}{\gamma P} = \frac{\kappa_T}{\gamma} \tag{16}$$

where κ is the isothermal compressibility. It can also be shown that for sonic flow to occur under isothermal conditions, the speed of sound, c_T, is equal to:

$$c_T^2 = \frac{R_g T}{M_w} = \left[\frac{\partial P}{\partial \rho}\right]_T = \frac{1}{\rho \kappa_T} \text{ where } \kappa_T = \frac{1}{P} \tag{17}$$

If we assume ideal gas behavior, we can calculate the mass flux and flow exit conditions under constant entropy and upstream enthalpy conditions using the nozzle flow equations developed earlier:

$$\rho_e = \rho_o \left(\frac{P_e}{P_o}\right)^{\frac{1}{\gamma}} \tag{18}$$

$$T_e = T_o \left(\frac{P_e}{P_o}\right)^{\frac{\gamma-1}{\gamma}} \tag{19}$$

$$u_e = \sqrt{u_o^2 + 2\left(\frac{\gamma}{\gamma-1}\right)\left(\frac{P_o}{\rho_o}\right)\left[1-\left(\frac{P_e}{P_o}\right)^{\frac{\gamma-1}{\gamma}}\right]} \tag{20}$$

$$G_e = \rho_e u_e = \sqrt{\underbrace{u_o^2\rho_o^2\left(\frac{P_e}{P_o}\right)^{\frac{2}{\gamma}}}_{u_o^2\rho_e^2} + \underbrace{2\left(\frac{\gamma}{\gamma-1}\right)(P_o\rho_o)\left[\left(\frac{P_e}{P_o}\right)^{\frac{2}{\gamma}} - \left(\frac{P_e}{P_o}\right)^{\frac{1+\gamma}{\gamma}}\right]}_{2\rho_e^2(h_o-h_e)}} \tag{21}$$

$$\tag{22}$$

Note that the mass flux is expressed as a function of upstream conditions and exit pressure P_e only. There exists a unique value of P_e that leads to a maximum in mass flux as illustrated in Figure 1. The exit pressure at which the mass flux is maximized in Figure 1 is 4.84 barg with a corresponding mass flux of approximately 2200 $\mathrm{kg/m^2/s}$.

It can be shown that the mass flux is always maximized at critical value of P_e. Where P_e is greater than the ambient back pressure, P_b, the flow is choked or sonic:

$$P_e = P_o\left(\frac{2}{\gamma+1}\right)^{\frac{\gamma}{\gamma-1}} \geq P_b \tag{23}$$

$$T_e = T_o\left(\frac{2}{\gamma+1}\right) \tag{24}$$

where P_b is the ambient back pressure and P_e is the critical flow pressure. Under these conditions the mass flux is not influenced by the ambient back pressure up to P_e and the flow is said to be choked or sonic. The value of P_e/P_o from Equation 23 can be substituted in Equation 21 to yield the maximum mass flux without trial and error. If $P_e = P_b$ then the flow is said to be unchoked or subsonic and the maximum mass flux is obtained by substituting P_e in Equation 21 with P_b.

Choked flow for ideal gases is only possible if the upstream pressure P_o is approximately two times the value of the back pressure, or $P_e/P_o \simeq 0.55$. For the specific case of nitrogen flow illustrated

Figure 1: Mass flux vs. exit pressure for nitrogen. $T_o = 100$ °C, $P_o = 10$ barg, $u_o = 0$ m/s

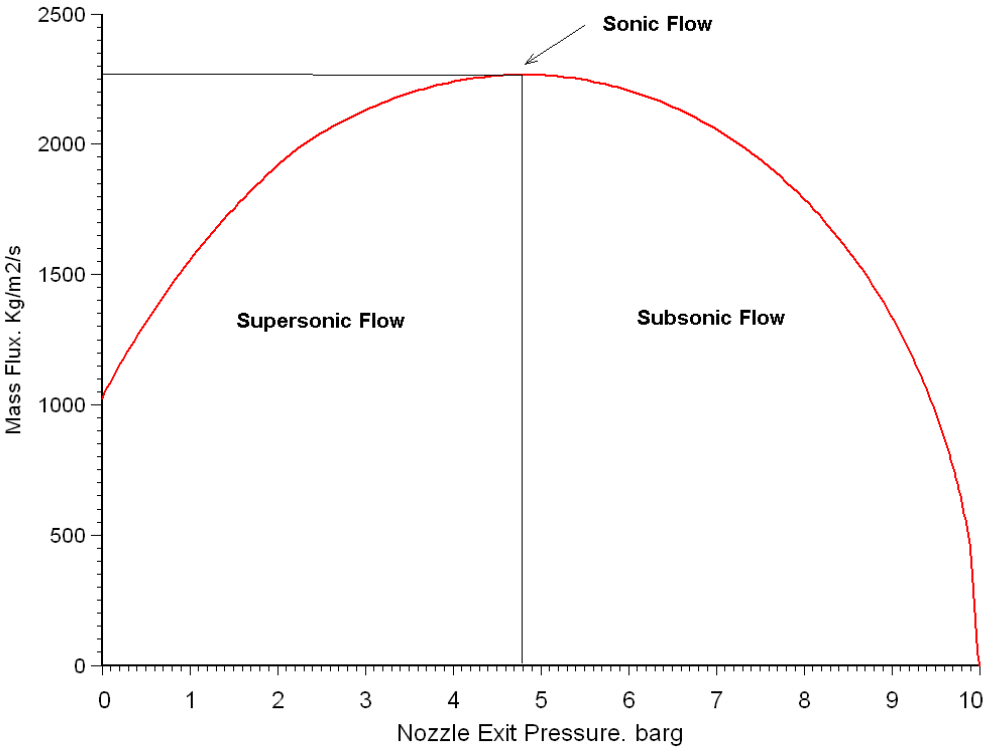

Source: SuperChems Expert

in Figure 1:

$$\rho_o = \frac{P_o M_w}{R_g T_o} = \frac{11 \times 10^5 \times 28}{8314 \times 373} = 9.932 \text{ kg/m}^3 \tag{25}$$

$$\gamma = \frac{C_p}{C_v} = 1.4 \tag{26}$$

$$\frac{P_e}{P_o} = \left(\frac{2}{\gamma+1}\right)^{\frac{\gamma}{\gamma-1}} = \left(\frac{2}{1.4+1}\right)^{\frac{1.4}{1.4-1}} = \left(\frac{2}{2.4}\right)^{3.5} = 0.528 \tag{27}$$

$$G_e = \sqrt{0 + 2 \times \frac{1.4}{1.4-1} \times 11 \times 10^5 \times 9.932 \left[0.528^{\frac{2}{1.4}} - 0.528^{\frac{2.4}{1.4}}\right]} \tag{28}$$

$$= \sqrt{2 \times 3.5 \times 10925200 \times [0.40157 - 0.33459]} = 2263.18 \text{ kg/m}^2/\text{s} \tag{29}$$

The mass flow rate can be calculated directly from the mass flux and nozzle flow area. A discharge coefficient is typically used to account for the irreversible flow losses caused by the nozzle entrance shape. A well rounded nozzle discharge coefficient C_d will approach a value of one, typically 0.95. If the upstream velocity is zero and the flow is subsonic:

$$\frac{dm_{out}}{dt} = C_d A_e \sqrt{2 P_o \rho_o \left(\frac{\gamma}{\gamma-1}\right) \left[\left(\frac{P_b}{P_o}\right)^{2/\gamma} - \left(\frac{P_b}{P_o}\right)^{\frac{\gamma+1}{\gamma}}\right]} \tag{30}$$

Under choked flow conditions, the mass flow rate is calculated from a simplified form of Equation 21 which incorporates the critical pressure ratio P_e/P_o from Equation 23:

$$\frac{dm_{out}}{dt} = C_d A_e \sqrt{\gamma P_o \rho_o \left(\frac{2}{\gamma+1}\right)^{\frac{\gamma+1}{\gamma-1}}} \tag{31}$$

6 vdP Integration

Another popular and robust form of Equation 4 involves vdP integration. This form is less prone to errors associated with phase change and vapor quality for multiphase flow. The enthalpy change, dh, can be related to specific volume and entropy:

$$dh = Tds + vdP = Tds + \frac{dP}{\rho} \tag{32}$$

For isentropic flow, $ds = 0$, and the dh term can be replaced with vdP or $\frac{dP}{\rho}$. As a result:

$$G_e = \rho_e \sqrt{2\int_{P_e}^{P_o} vdP + u_o^2} = \rho_e \sqrt{2\int_{P_e}^{P_o} \frac{1}{\rho} dP + u_o^2} \tag{33}$$

For liquid flow with a constant liquid density or liquid specific volume, Equation 33 can be reduced to the well known Bernoulli flow equation:

$$G_e = \rho \sqrt{\frac{2}{\rho}(P_o - P_e) + u_o^2} = \sqrt{2\rho(P_o - P_e) + \rho u_o^2} \tag{34}$$

or

$$\frac{dm_{out}}{dt} = \dot{m}_{out} = A_e G_e C_d = A_e C_d \sqrt{2\rho(P_o - P_e) + \rho u_o^2} \tag{35}$$

We note from Equation 33 that $\int vdP$ can be easily evaluated without the use of complex equations of state if we can provide a simple expression of how v or ρ changes with pressure using a specific thermodynamic path.

This observation is what sparked the development of the omega method and later developments of reduced analytical models. Essentially, the omega method and reduced analytical models are simplified equations of state that are only valid for a specific pressure range and for a specific thermodynamic path temperature range.

7 Twophase Flow Implications

A variety of scenarios can lead to twophase flow under relief conditions including but not limited to, (a) poor vapor/liquid disengagement geometries, (b) foamy and/or viscous fluids, (c) liquid swell due to bubbles generation and/or runaway reactions, (d) fluid expansion due to heating, (e) high superficial vapor velocity (oversized relief device), (f) entrainment due to gas sparging, and/or (g) condensation in the relief discharge line.

It is preferred to eliminate or to significantly reduce the likelihood of twophase flow. Twophase flow can lead to high potential toxicity, thermal, and overpressure hazard footprints from discharges to atmosphere. As a result, additional vent containment and flow separation may be required to manage or reduce the risks of twophase flow. This is particularly challenging because energy tempering does not occur for homogeneous twophase flow during twophase relief. Twophase flow often leads to large relief requirements and large relief devices. Large relief requirements may make it impractical to to use a relief device as the only means of safeguarding.

Extensive information is required for pressure relief systems design/evaluation including but not limited to, (a) flow type including non-equilibrium, subcooled, liquid, twophase, supercritical, and vapor, (b) piping and fittings inlet pressure loss (relief device performance), (c) piping and fittings backpressure (relief device performance), (d) discharge mass flow rate, quality, composition, temperature, and pressure, slip ratio, (e) location of choke points and reaction forces, (f) slug formation and piping vibration risks, and (g) thermodynamic, physical, and transport properties.

Methods for calculating twophase flow are therefore complex and can be time consuming when evaluating a large number of relief scenarios, especially for systems involving runaway reactions, or systems containing a large number of chemicals. This is one of the main reasons for why numerous publications focused on the development of simplified methods for the estimation of twophase flow have appeared in the open literature over the last several decades.

A simple method that is widely used is the omega method.

8 The Omega Method

Instead of using a detailed equation of state to represent the PvT and phase equilibrium behavior of pure components and/or mixtures, a simple two-parameter equation of state (reduced analytical model) is used with two adjustable parameters, a and b. The a and b parameters are regressed/calculated from a best fit of either isentropic or isenthalpic equilibrium flash calculations:

$$\frac{\rho_o}{\rho} - 1 \;=\; a\left(\frac{P_o}{P} - 1\right) + b\left(\frac{P_o}{P} - 1\right)^2 \tag{36}$$

The parameters a and b are obtained by fitting the volumetric expansion behavior using two or more flash equilibrium calculations at pressures lower than the stagnation conditions. This approach may not work well for mixtures with wide boiling point differences such as heavy hydrocarbon mixtures containing hydrogen, for example. The same concept can be extended to pipe flow using homogeneous equilibrium (no slip between the liquid and vapor phases).

Leung's [3] simplification of the two-parameter equation (Equation 36), "the omega method", was introduced in several publications with an overall summary paper published in Chemical Engineering Progress in December of 1996 [4]. Leung uses Equation 36 with $b = 0$ and $a = \omega$:

$$\frac{\rho_o}{\rho} - 1 = \omega \left(\frac{P_o}{P} - 1 \right) \tag{37}$$

This simplification leads to a generalized form for mass flux for nozzle flow using the ω pressure/volume relationship as defined in Equation 37:

$$\frac{G_e}{\sqrt{P_o \rho_o}} = \frac{\sqrt{-2\left[\omega \ln\left(\frac{P_e}{P_o}\right) + (\omega - 1)\left(1 - \frac{P_e}{P_o}\right)\right]}}{1 + \omega\left(\frac{P_o}{P_e} - 1\right)} \tag{38}$$

This equation can be evaluated for different ratios of P_e/P_o to find the point at which G_e is maximum where P_e ranges from the stagnation conditions to whatever back pressure, P_b, is imposed on the flow system. The critical pressure ratio can also be solved for by setting the first derivative of G_e with respect to pressure to 0. This is illustrated in Figure 2.

Figure 2: The omega method for estimation of twophase mass flux and critical pressure ratio. Taken from Chemical Engineering Progress [4]

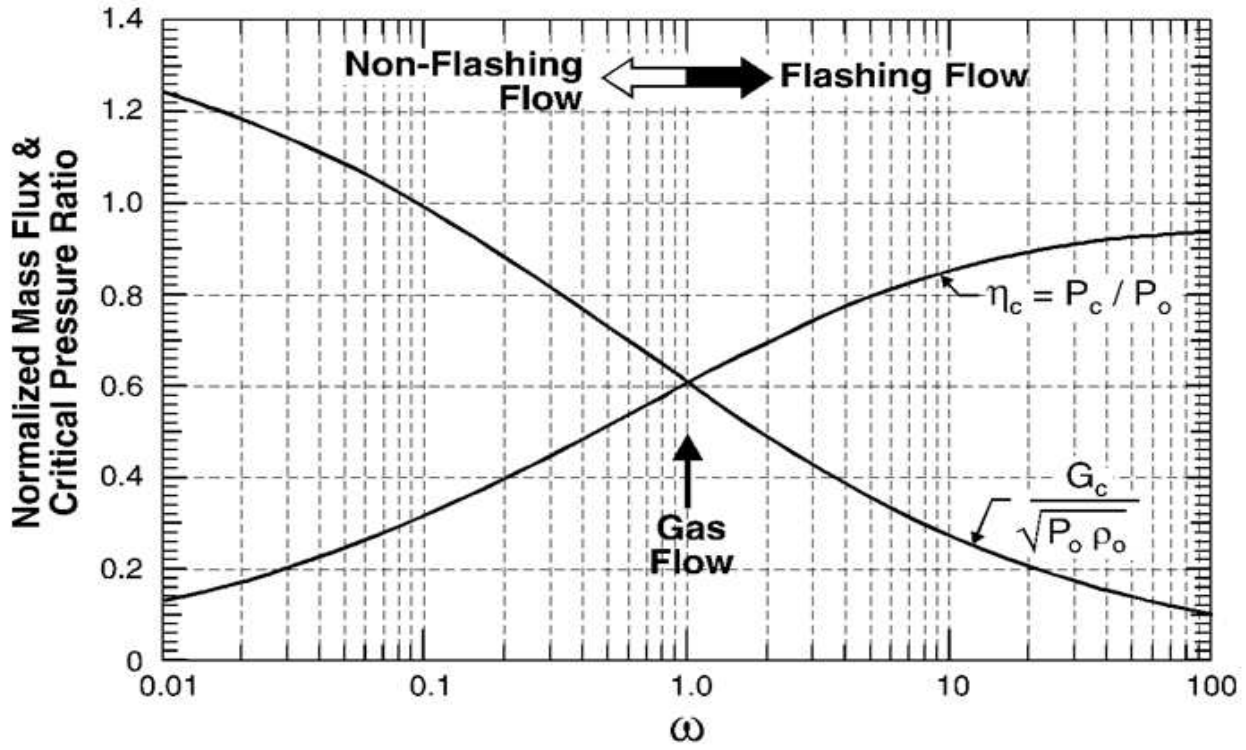

Simpson [5] developed an approximation of the solution for P_e/P_o that will maximize G_e as a function of ω:

$$\frac{P_e}{P_o} \simeq \left[1 + \left(1.0446 - 0.0093431\omega^{0.5}\right)\omega^{-0.56261}\right]^{(0.014685\ln(\omega)-0.70356)} \tag{39}$$

The value of ω ranges from 0 for all liquid flow, 1 for all vapor/gas flow, greater than 1 for flashing flow and between 0 and 1 for non-flashing flow. The ω method is simple to evaluate for systems involving pure components and is of limited use for systems involving mixtures with wide boiling point differences or where composition changes are significant due to chemical reaction or large pressure changes.

In addition, recent experimental flow data indicate that slip should be considered in the estimation of mass flux, especially for viscous systems [6, 7]. This becomes an issue when designing downstream effluent handling equipment since the assumption of no slip between the liquid and the vapor phases can lead to underestimation of the twophase mass flux and as a result an overestimate of the required relief area.

Leung [3] provides the following expressions for ω, which depend on stagnation properties only.

Flashing systems:

$$\omega = \alpha_o + (1-\alpha_o)\rho_o c_p T_o P_o \left(\frac{v_{v,o} - v_{l,o}}{h_{v,o} - h_{l,o}}\right)^2 \tag{40}$$

where α_o is the volumetric void fraction at stagnation conditions.

Non-flashing systems:

$$\omega = \alpha_o \tag{41}$$

Leung [3] published many variations of the omega method extending its use to pipe flow, subcooled flow and for the calculation for reaction forces. We find these extensions less useful since they cannot easily handle inlet piping and outlet piping configuration with multiple segments and fittings. The geometry of the inlet and outlet piping becomes very important for flashing flow, since pressure drop will lead to a location specific vapor quality change and will lead to choking at lower mass flow rates. For flashing flow, choking is location and geometry specific [6].

9 Omega Method Advantages and Disadvantages

The omega method became popular because of its simplicity, especially for twophase flow. The use of an analytical form to represent density as a function of pressure enabled easy and quick estimation of twophase mass flux. Although trial and error is required to find the mass flux and critical pressure ratio, an omega chart can be used to quickly locate the solution (see Figure 2). The

Table 1: Limitations on use of the omega method published in ISO 4126-10 [9]

Category	Limit
Flashing flow	$\frac{T}{T_c} < 0.9$, $\frac{P}{P_c} < 0.5$
Flashing flow for mixtures	Normal boiling point range (NBP) < 100 K
Omega value	$0 \leq \omega \leq 100$, at $\frac{P}{P_o} = 0.9$
Dissolved gases	Do not use
Viscosity	< 100 cp
Temperature rise rate	$\frac{dT}{dt} < 2$ K/s
Pressure rise rate	$\frac{dP}{dt} < 12$ bar/min
Immiscible liquids	Do not use

omega method also featured the use of a limited set of physical properties at the stagnation conditions. Several forms of the omega method were published to enable subcooled flow calculations for nozzles and pipe flow.

Because of its simplicity, the omega method has many disadvantages but continues to be used despite its limitations [8, 9, 10, 11, 12]. The estimation of the omega parameter for mixtures with wide boiling point differences leads to erroneous estimation of flow rate as shown by Melhem (see [8] and [11]). Most reaction systems involve mixtures with wide boiling point differences. Significantly wide boiling point differences can be associated with gassy and hybrid systems. Many reaction systems involve supercritical components as well, or include reactants that become supercritical during the reaction process.

Multiple omega equations forms and exceptions are required to properly and broadly apply the omega method leading to added complexity when considering non-equilibrium flow, subcooled flow, vertical or inclined twophase flow in piping, high viscosity flow, and/or flows where multiple chokes are possible.

Estimation of the correct omega parameter for a mixture requires regression of density vs. pressure using detailed flash calculations. At least one additional point at $P_e/P_o = 0.9$ is required in addition to the stagnation conditions. Furthermore, additional flash calculations are required to develop the omega parameter for flow estimates downstream from the nozzle.

As a result, one has to question the usefulness of the omega method since the generation of multiple flash points can easily be used to develop a numerical vdP integral instead with many less limitations and without introducing additional regression errors.

The International Organization for Standardization (ISO) [9] published omega method limitations and restrictions in "Part 10 of ISO-4126: Sizing of safety valves for gas/liquid twophase flow" as shown in Table 1.

Guidance is not provided by ISO 4126-10 [9] on how to calculate the mixture critical pressure P_c

and mixture critical temperature T_c. A simple molar averaged value should not be used. An equation of state with adequate mixing and combining rules is required to calculate accurate mixture critical properties.

The omega method can be used for single component flow estimates within the proposed limits. However, the omega method should not be used for multicomponent systems and/or reaction systems unless the omega parameter is regressed from flash calculations that consider retrograde and phase changes at a sufficient number of pressure points.

10 Generalized Direct vdP Integration

The methods outlined above for the estimation of mass flux are enthalpy based. These methods require the use of an accurate equation of state to represent enthalpy. The mass flux is calculated by maximizing $G = \rho u = \rho\sqrt{2\Delta h + u_o^2}$ as shown in Equation 4 where u_o is the nozzle initial approach velocity.

For a multicomponent mixture twophase flow through a nozzle, an isentropic thermodynamic path is assumed and several flash computations are performed at reduced pressures to estimate twophase density and vapor quality. Flash calculations are performed at successively lower pressures than the source pressure until mass flux is maximized. The twophase mixture density, flash fraction, viscosity, and slip ratio are calculated as a function of pressure. The mass flux is then obtained by maximizing the following expression for mass flux:

$$G_e = \rho_{m,t}\sqrt{-2\int_{P_o}^{P_t}\frac{dP}{\rho} + u_o^2} \tag{42}$$

where the subscript t refers to the throat of a relief device or flow orifice and $_m$ refers to a mixture property. A generalized expression of Equation 42 can be written including slip at the throat [13]:

$$G_e^2 = \frac{-2\int_{P_o}^{P_t}\left[\frac{x}{\rho_v} + \frac{1-x}{\rho_l}\right]dP + u_o^2}{\left[\frac{x_t}{\rho_{v,t}u_{r,t}} + \frac{1-x_t}{\rho_{l,t}}\right]^2\left[x_t u_{r,t}^2 + 1 - x_t\right]} \tag{43}$$

where x is the vapor quality or mass fraction, u_r is the slip ratio, $_v$ designates a vapor or gas phase, and $_l$ designates a liquid phase. Direct vdP integration (Equation 42) provides significant advantages over the omega method. One simple form is required for nozzle flow and can be easily extended to pipe flow. This method can be applied to mixtures, reaction systems, and pure components without limits on temperature, pressure, and composition. Direct vdP integration can provide discharge temperature and composition data for use in downstream equipment sizing and dispersion analysis. It can be estimated using a spreadsheet or a simple computer program where the user is able to supply the flash calculations at multiple pressure points [8, 11, 12].

The direct integration method should be used instead of the omega method because it is simpler, consists of one equation, has many less exceptions than the omega method, covers a wide variety of flow types, as well as broader temperature, pressure and composition ranges. The vdP integration is typically performed using discrete pressure steps as described in Section 2.

No one invented vdP integration. The vdP integral shown in Equation 33 has always been there since the declaration of the first law of thermodynamics!.

11 Nozzle Flow Slip Ratio, u_r

For the case where the vapor and liquid phases are traveling at different velocities, the twophase mixture density is expressed as a function of the void fraction, α, and the slip ratio, $u_r = u_v/u_l$:

$$\rho_m = \alpha\rho_v + (1-\alpha)\rho_l = \frac{x + (1-x)u_r}{\frac{x}{\rho_v} + \left(\frac{1-x}{\rho_l}\right)u_r} \tag{44}$$

The twophase mass flux with slip is also expressed in terms of the void fraction:

$$G_m = G_v + G_l = \rho_m u_m = \rho_v u_v \alpha + \rho_l u_l (1-\alpha) = \frac{\rho_v u_v \alpha}{x} = \frac{\rho_l u_l\,(1-\alpha)}{1-x} \tag{45}$$

Replacing α in the above equation by:

$$\alpha = \frac{x\rho_l}{x\rho_l + (1-x)\rho_v u_r} = \frac{\rho_m - \rho_l}{\rho_v - \rho_l} \tag{46}$$

leads to the following expression for G_m:

$$G_m = \left[\frac{x}{\rho_v u_v} + \frac{1-x}{\rho_l u_l}\right]^{-1} \tag{47}$$

Assuming an isentropic thermodynamic path to calculate the flash fraction, the energy equation yields the following expression for phase velocities:

$$x u_v^2 + (1-x)u_l^2 = 2\Delta h = 2\left[h_o - x h_{e,v} - (1-x)h_{e,l}\right] \tag{48}$$

We seek to maximize the twophase mass flux as a function of the slip ratio, i.e.:

$$\frac{dG_m}{du_r} = 0 \tag{49}$$

Since Δh and x are constants at the specified thermodynamic path, we will differentiate a mathematically simpler expression instead:

$$\frac{d}{du_r}\left[\frac{2\Delta h}{G_m^2}\right] = 0 \tag{50}$$

where:

$$\frac{2\Delta h}{G_m^2} = \left[xu_r^2 + 1 - x\right]\left[\frac{x}{\rho_v u_r} + \frac{1-x}{\rho_l}\right]^2 = \frac{1}{\rho_{m,t}^2} \tag{51}$$

where the subscript t refers to the throat of a nozzle or a relief device. Setting the derivative of the above expression to 0 yields the following expression:

$$x(1-x)\left[\frac{u_r}{\rho_l} - \frac{1}{u_r^2\rho_v}\right]\left[\frac{x}{\rho_v u_r} + \frac{1-x}{\rho_l}\right] = 0 \tag{52}$$

The only nontrivial solution to this equation is:

$$\frac{u_r}{\rho_l} - \frac{1}{u_r^2\rho_v} = 0 \tag{53}$$

or

$$u_r = \left(\frac{\rho_l}{\rho_g}\right)^{1/3} \tag{54}$$

Equation 54 is often referred to in the literature as Moody slip. It can also be shown that $u_r = \left(\frac{\rho_l}{\rho_g}\right)^{1/2}$ when the momentum balance is used instead of the energy balance. This is referred to in the literature as Fauske slip.

It is interesting to note that Equation 43 implies a throat twophase density that is different from the twophase density expression shown in Equation 44 when the slip ratio is greater than 1:

$$\rho_{m,t} = \frac{1}{\left[\frac{x_t}{\rho_{v,t}u_{r,t}} + \frac{1-x_t}{\rho_{l,t}}\right]\sqrt{\left[x_t u_{r,t}^2 + 1 - x_t\right]}} \tag{55}$$

or

$$\frac{\rho_{Eq44}}{\rho_{Eq55}} = \left[\frac{x + u_r - u_r x}{u_r}\right]\sqrt{xu_r^2 + 1 - x} \tag{56}$$

Table 2: Twophase Reduced Analytical Models

Model	Points	Empirical Model Equation
A and ω	2	$\frac{v}{v_A} - 1 = \alpha\left(\frac{P_A}{P} - 1\right)$
B	3	$\frac{v}{v_A} - 1 = \alpha\left(\frac{P_A}{P} - 1\right)^{\beta}$
C	3	$\frac{v}{v_A} - 1 = \alpha\left(\left[\frac{P_A}{P}\right]^{\beta} - 1\right)$
D	3	$\frac{v}{v_A} - 1 = \alpha\left(\frac{P_A}{P} - 1\right) + \beta\left(\frac{P_A}{P} - 1\right)^2$
E	2	$x = a_0 + a_1 P$ $\frac{1}{v_g} = b_0 P^{b_1}$ $\frac{1}{v_f} = c_0 + c_1 P$
F	3	$x = a_0 + a_1 P + a_2 P^2$ $\frac{v_g}{v_{gA}} - 1 = b_0\left[\left(\frac{P_A}{P}\right)^{b_1} - 1\right]$ $\frac{1}{v_f} = c_0 + c_1 P + c_2 P^2$

The two phase specific volume is: $v = xv_g + (1-x)v_f$. Equations are fit at an upstream saturated condition P_A and possibly a second point P_B and even a third P_C point. Note that g indicates gas phase, f indicates liquid phase, and x vapor quality or mass fraction vapor.

12 Simple Reduced Analytical Models

A simple reduced analytical model (see Simpson [13]) can be established where a twophase density form is fit as a function of pressure as shown in Table 2. These reduced analytical forms employ typically one, two, or three parameters. It is important to note that while reduced analytical density models integration methods yield a very good estimate of mass flux for pure components they may not provide an accurate estimate of critical flow (choked flow) pressure, temperature, and vapor quality at the exit conditions (see Melhem [8, 11, 12]).

Melhem [8, 11, 12] showed that mass flux estimates for mixtures with wide boiling point ranges can be significantly underestimated. As a result, reduced analytical models are not recommended for mixtures with wide boiling point differences or reacting mixtures. In addition, for flows in piping systems involving relief devices and/or flow area changes such as reduction and expansion, reduced analytical density models must be fit for the inlet line (high pressure) and the discharge line (low pressure) in order to produce reasonable estimates of mass flux.

Simpson [13] also extended the use of these reduced analytical models to twophase pipe flow using empirical equations fitting viscosity as a function of pressure.

13 Complex Reduced Analytical Models

The use of reduced analytical density (PvT) models for nozzle flow mass flux integration can provide some advantages when dealing with mixtures containing a large number of components.

Reasonable estimates of flow rates and choke points can be achieved with a significant reduction in computational time, especially for extensive dynamic simulations.

SuperChems Expert uses multiple series of reduced analytical models regressed from detailed flash calculations for separated flows. The multiple series of reduced analytical models significantly reduces the computational time for 1D and 2D fluid dynamics simulation where the computational domains are divided into hundreds or thousands of computational nodes.

We consider two models proposed by Simpson [13] for homogeneous and separated flows:

Homogeneous Flow:

$$\frac{v_m}{v_o} = \frac{\rho_o}{\rho_m} = 1 + a\left[\left(\frac{P_o}{P}\right)^b - 1\right] \tag{57}$$

$$\frac{T_m}{T_o} = 1 + a^{'}\left[\left(\frac{P}{P_o}\right)^{b^{'}} - 1\right] \tag{58}$$

Separated Flow:

$$\frac{v_g}{v_{g,o}} = \frac{\rho_{g,o}}{\rho_g} = 1 + a\left[\left(\frac{P_o}{P}\right)^b - 1\right] \tag{59}$$

$$\frac{T_g}{T_{g,o}} = 1 + a^{'}\left[\left(\frac{P}{P_o}\right)^{b^{'}} - 1\right] \tag{60}$$

$$\frac{1}{v_l} = \rho_l = c_0 + c_1 P + c_2 P^2 \tag{61}$$

Homogeneous and Separated Flows:

$$v = \frac{1}{\rho} \tag{62}$$

$$v_m = x v_g + (1 - x)\, v_l \tag{63}$$

$$x = a_0 + a_1 P + a_2 P^2 \tag{64}$$

$$\mu_m = \alpha \mu_g + (1 - \alpha)\, \mu_l = d_0 + d_1 P + d_2 P^2 \tag{65}$$

$$\alpha = \frac{\rho_m - \rho_l}{\rho_g - \rho_l} = \frac{x \rho_l}{x \rho_l + (1 - x)\, \rho_g S} \tag{66}$$

$$S = \zeta \left(\frac{\rho_l}{\rho_g}\right)^{\eta} \tag{67}$$

ζ is typically 1.0 and η ranges from 1/3 to 1/2 for slip flow and equals 0 for constant slip or homogeneous flow. x is the mass fraction of vapor, v is the fluid specific volume, ρ is the fluid mass density, α is the flowing vapor void fraction with slip where applicable, μ is the fluid viscosity. The subscript o designates initial source conditions, l designates liquid, m designates mixture, g designates vapor or gas, and t designates the nozzle throat. a, b, c and d are parameters that are regressed

to represent mixture final conditions, typically at $0.75P_o$, $0.5P_o$, and ambient pressure. An isentropic thermodynamic path is often selected, although other paths such as isenthalpic, isothermal, and/or constant volume can be selected as well.

Integrating $v_m(P)$ from the source pressure P_o to a nozzle throat pressure P_t can be performed analytically to yield:

$$\int_{P_o}^{P_t} v_m dP = P_t v_o \left[1 - a - \left(\frac{a}{b-1}\right)\left(\frac{P_o}{P_t}\right)^b\right] - P_o v_o \left[1 - a - \frac{a}{b-1}\right] \quad \text{where } b \neq 1 \tag{68}$$

$$= v_o (1-a)(P_t - P_o) + v_o a P_o \ln\left(\frac{P_t}{P_o}\right) \quad \text{where } b = 1 \tag{69}$$

In addition, an implicit speed of sound estimate can be obtained analytically as well at any value of nozzle throat pressure:

$$c_s = \sqrt{\left(\frac{\partial P}{\partial \rho}\right)_s} = \frac{v_m}{v_o}\sqrt{\frac{v_o P_t}{ab\left(\frac{P_o}{P_t}\right)^b}} = v_m\sqrt{\frac{P_t}{abv_o\left(\frac{P_o}{P_t}\right)^b}} = v_m\sqrt{\frac{P_t^{1+b}}{abv_o P_o^b}} \tag{70}$$

For a polynomial expression of density as a function of pressure, $\frac{1}{v_l} = \rho_l = c_0 + c_1 P + c_2 P^2$, the speed of sound is simply:

$$c_s = \sqrt{\frac{1}{2P_t c_2 + c_1}} \tag{71}$$

and the mass flux is:

$$\int_{P_o}^{P_t} v_l dP = \int_{P_o}^{P_t} \frac{1}{\rho_l} dP = \int_{P_o}^{P_t} \frac{dP}{c_0 + c_1 P + c_2 P^2} \tag{72}$$

$$= \frac{2}{\sqrt{c_3}}\left[\arctan\left(\frac{2P_t c_2 + c_1}{\sqrt{c_3}}\right) - \arctan\left(\frac{2P_o c_2 + c_1}{\sqrt{c_3}}\right)\right] \quad \text{where } c_3 > 0 \text{ or,} \tag{73}$$

$$= \frac{2}{\sqrt{-c_3}}\left[\log\frac{2c_2 P_t + c_1 - \sqrt{-c_3}}{2c_2 P_t + c_1 + \sqrt{-c_3}} - \log\frac{2c_2 P_o + c_1 - \sqrt{-c_3}}{2c_2 P_o + c_1 + \sqrt{-c_3}}\right] \quad \text{where } c_3 < 0 \tag{74}$$

$$c_3 = 4c_0 c_2 - c_1^2 \tag{75}$$

The reduced analytical models presented above are used with the following general expression of nozzle mass flux to locate the throat pressure that leads to a maximum value in mass flux:

$$G^2 = \rho_{m,t}^2\left(2\Delta h + u_o^2\right) = \frac{-2\int_{P_o}^{P_t} v_m dP + u_o^2}{\underbrace{\left[\frac{x_t}{\rho_{g,t} u_{r,t}} + \frac{1-x_t}{\rho_{l,t}}\right]^2 \left[x_t u_{r,t}^2 + 1 - x_t\right]}_{\left(\frac{1}{\rho_{m,t}}\right)^2}} \tag{76}$$

$$= 2\rho_{m,t}^2 \int_{P_t}^{P_o} v_m dP + \rho_{m,t}^2 u_o^2 \tag{77}$$

where h is the fluid specific enthalpy, $u_{r,t} = \frac{u_g}{u_l}$ is the slip ratio at the throat pressure and temperature conditions, and u_o is the nozzle entrance velocity, typically 0 for vessel flow.

It is interesting to note that equation 57 is a single parameter ω equation when $b = 1$. As a result, given a nozzle throat pressure P_t, the mass flux and speed of sound can be calculated as follows:

$$c_{s,t} = v_m \sqrt{\frac{P_t^2}{a v_o P_o}} \tag{78}$$

$$G^2 = -2\rho_m^2 \left[v_o (1-a)(P_t - P_o) + v_o a P_o \ln\left(\frac{P_t}{P_o}\right) \right] + \rho_m^2 u_o^2 \tag{79}$$

For all liquid flow, $a \to 0$. For all vapor flow, $a \to 1$. $0 < a < 1$ for non-flashing flow and $a > 1$ for flashing flow.

Reduced PvT models also provide an advantage when solving 1D fluid dynamics equations, especially for flow related boundary conditions. A required flow boundary condition is conservation of stagnation enthalpy across the flow boundary:

$$h_1 + \frac{1}{2}u_1^2 = h_2 + \frac{1}{2}u_2^2 \tag{80}$$

$$h_1 - h_2 = \frac{1}{2}\left(u_2^2 - u_1^2\right) \tag{81}$$

Under isentropic flow conditions, $dh = vdP$:

$$h_1 - h_2 = -\int_{P_1}^{P_2} v dP = \int_{P_2}^{P_i} v dP - \int_{P_1}^{P_i} v dP = \frac{1}{2}\left(u_2^2 - u_1^2\right) \tag{82}$$

where P_i the maximum reduced PvT model pressure. For liquid systems with constant liquid density, this boundary condition reduces to:

$$P_1 + \frac{1}{2}\rho u_1^2 = P_2 + \frac{1}{2}\rho u_2^2 \tag{83}$$

If flow boundary 1 is a vessel where $u_1 = 0$, then:

$$P_1 = P_2 + \frac{1}{2}\rho u_2^2 \tag{84}$$

Equations 57 and 58 can be differentiated with respect to pressure for use in integration calculations

for pipe flow:

$$\frac{\partial v_m}{\partial P} = -\frac{v_o a b}{P}\left(\frac{P_o}{P}\right)^b \tag{85}$$

$$\frac{\partial \rho_m}{\partial P} = \frac{\rho_m^2}{\rho_o}\frac{ab}{P}\left(\frac{P_o}{P}\right)^b = -\rho_m^2\frac{\partial v_m}{\partial P} \tag{86}$$

$$\frac{\partial T_m}{\partial P} = \frac{T_o a' b'}{P}\left(\frac{P}{P_o}\right)^{b'} \tag{87}$$

14 Case Studies for Nozzle Flow

The final conditions for nozzle flow are usually determined using an isentropic thermodynamic flow path. The final pressure, temperature, phase, and composition are those at which mass flow is maximized [11, 8].

Figure 3 illustrates the nozzle isentropic thermodynamic flow path for the mixture of ethylene and butyl acrylate at different starting temperatures and 2000 psig. As the starting temperature is decreased the choke point phase of maximum flow shifts from vapor, to two phase, and then to saturated liquid. Note that at the 50 C starting condition the flow path goes through the critical point and ends up close to the bubble point boundary in the two phase region. We also note that the final choking temperature for highly subcooled liquid flow is very close to the value of the starting temperature since the liquid is only slightly compressible.

As the flow expands from the choke point to lower pressures, it is possible to cross the phase boundaries if the pressure is low enough. If the flow is expanding into a pipe with a larger flow area, it is possible to cross the phase boundaries and to have multiple chokes downstream of the first choke. For choked (sonic) flow, the flow is always regulated by the first choke. However, subsequent chokes typically occurring at area changes such as sudden expansions in the discharge piping, can reduce the capacity of a pressure relief valve due to the increase of backpressure.

If we increase the starting pressure to 30,000 psig for the ethylene-butyl acrylate mixture we notice that these starting conditions are well above the inversion curve for the mixture. An inversion curve represents the zero limit of the Joule-Thompson (JT) coefficient. At points above the inversion curve, a negative JT coefficient indicates that as the pressure is decreased the temperature should increase, while a positive JT coefficient indicates the opposite. It is a very good practice to establish an inversion curve for high pressure systems before attempting flow estimates.

This JT coefficient is expressed in terms of the change of temperature with respect to pressure at constant enthalpy, μ_H. At high pressures, negative values of μ_H indicate an increase in temperature for a constant enthalpy pressure drop. At low pressures, positive values of μ_H indicate a decrease

Figure 3: Isentropic nozzle flow for an ethylene-butyl acrylate mixture at 2000 psig

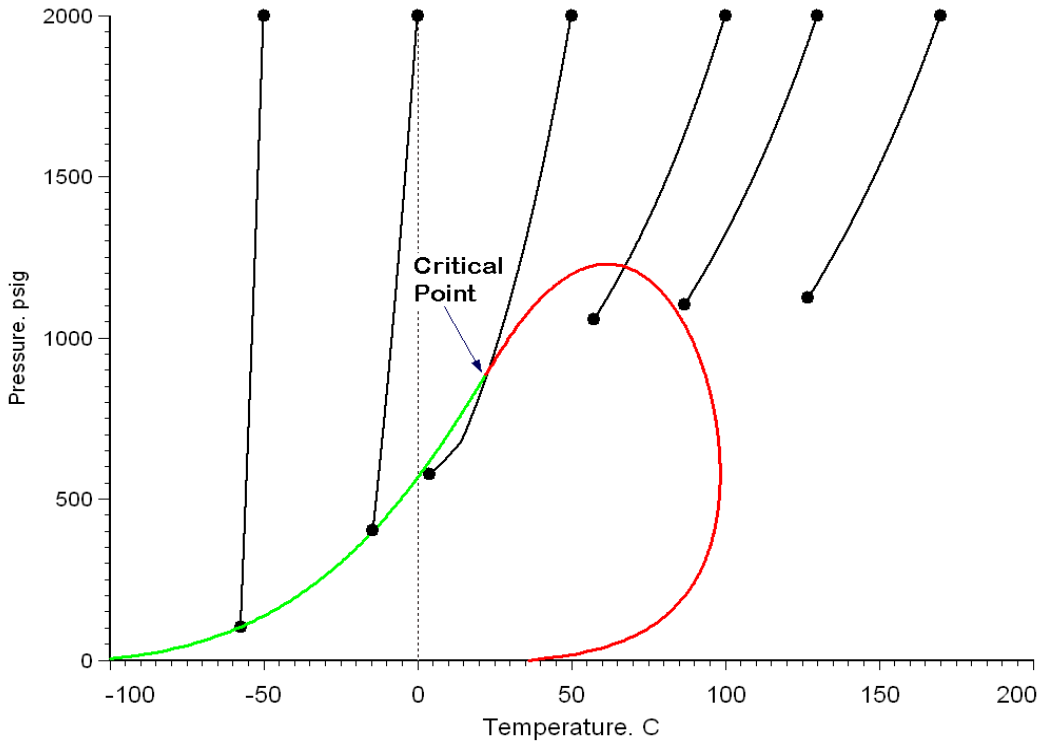

Source: SuperChems Expert

in temperature for a constant enthalpy pressure drop.

$$\mu_H = \left(\frac{\partial T}{\partial P}\right)_H = -\frac{1}{C_p}\left(\frac{\partial H}{\partial P}\right)_T = \frac{R_g T^2}{P C_p}\left(\frac{\partial Z}{\partial T}\right)_P = \frac{1}{C_p}\left[T\left(\frac{\partial V}{\partial T}\right)_P - V\right] \tag{88}$$

$$= \frac{1}{\rho C_p}(\beta T - 1) \tag{89}$$

where C_p is the molar real fluid heat capacity at constant pressure, V is the molar volume, and H is the molar enthalpy. Equation 89 can be used to construct a complete inversion curve, a curve that represents the locus of all the zero values of the Joule-Thompson coefficient. Figure 4 displays an inversion curve calculated by SuperChems Expert™ (a component of Process Safety Office®) using the Melhem modification of the Peng-Robinson equation of state [14, 15] for hydrogen.

Hydrogen is depressured using both an isenthalpic and an isentropic thermodynamics paths from 1500 psig and 100 C to the flow choke point. As shown in Figure 4, the isenthalpic path heats up to 100.6 C while the isentropic path cools down to 34.7 C. For an ideal gas, $\beta = 1/T$ and the Joule-Thompson coefficient is equal to 0. At critical conditions, it can be shown that μ_H will approach:

$$\mu_H \rightarrow \left(\frac{\partial T}{\partial P}\right)_\rho = \frac{\kappa_T}{\beta} \tag{90}$$

The inversion curve represents a severe test of the performance of an equation of state. Figure 5

Figure 4: Calculated inversion curve for hydrogen

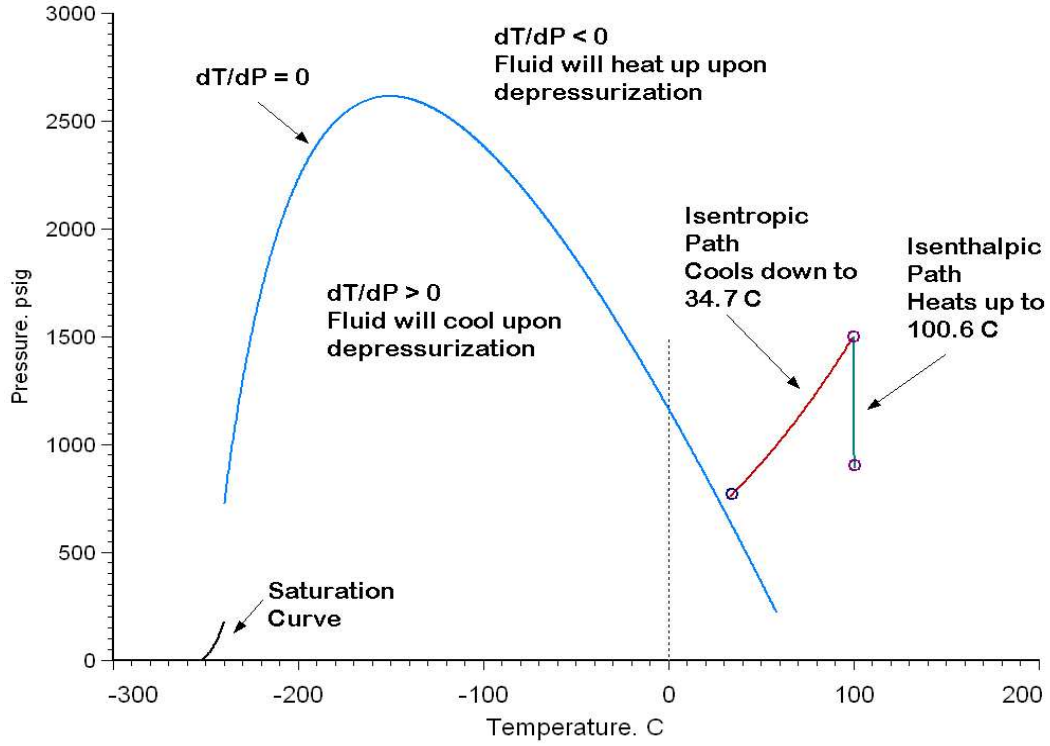

Source: SuperChems Expert

illustrates the impact of JT on the final temperature reached at choking conditions. For example, the temperature only drops from 200 C to approximately 140 C despite a pressure drop from 30000 psig to 9300 psig. This is attributed to the selected thermodynamic path for flow illustrated in Figure 5 which is isentropic for an ideal nozzle and not isenthalpic.

15 Case Studies for Pipe Flow

Unlike nozzle flow, the final conditions for pipe flow are determined by conserving stagnation enthalpy. The final pressure, temperature, phase, and composition are those at which the maximum possible flow can traverse the entire pipe and still reach the choke point at exactly the end of the pipe and/or the flow limiting element. In relief systems applications, choking typically occurs at the nozzle of a pressure relief valve, a control valve, or at a change of flow area in the piping system. Multiple chokes are possible if the starting pressure is high enough. For many applications, phase change will occur after the pressure expansion following the choke location.

For relief systems piping consisting of pipe segments and a pressure relief valve and/or a control valve, the flow through these devices is still established using isentropic flow because choking typically will occur at the valve nozzle. However, the approach velocity to the nozzle has to

Figure 5: Isentropic nozzle flow for an ethylene-butyl acrylate mixture at 5000, 10000, and 30000 psig

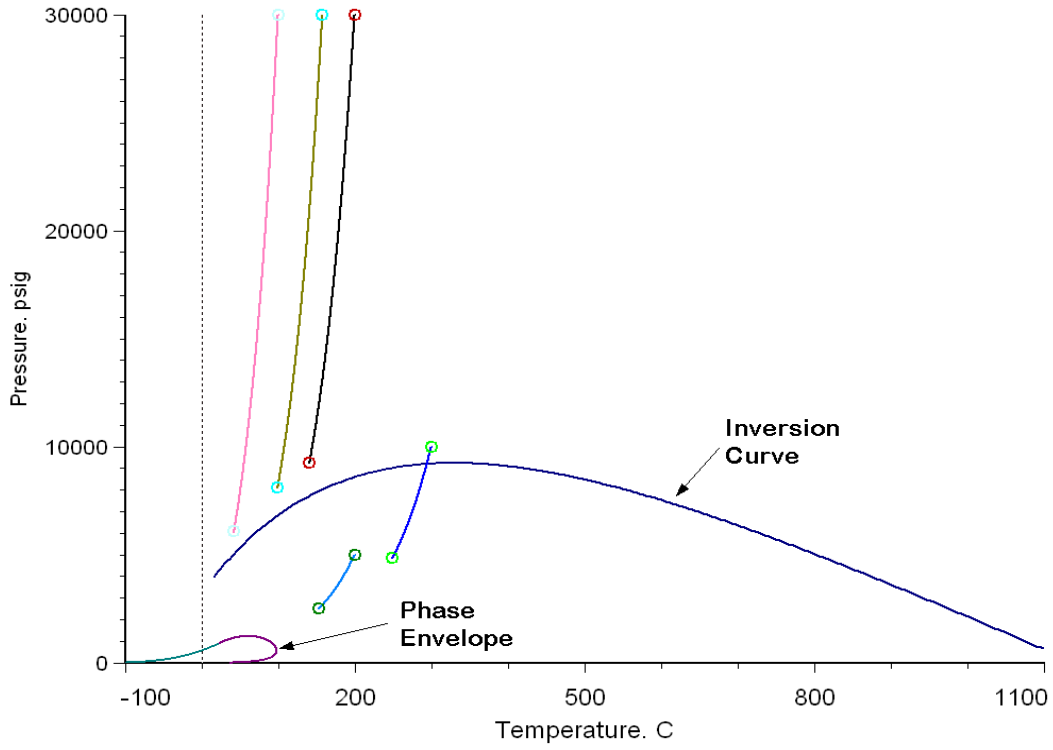

Source: SuperChems Expert

be accounted for when calculating stagnation enthalpy via an isentropic flow path. The piping flow solvers will try to push as much mass flow as possible through the relief systems piping, i.e. maximize flow that is possible through the piping. If the flow is choked at the relief device or control valve, the choke point is established iteratively until the maximum mass flow rate requested by the pipe solvers matches the one established by the nozzle solvers. This method is the method of choice where multiple chokes are possible [16].

We consider the flow of pure ethylene from a relief line with a short 1 m inlet line (3 inch), a 10 m discharge line (4 inch), and a 3K4 pressure relief valve. The starting conditions are 100 barg and 10 °C. As illustrated in Figure 6 the flow chokes at the two phase boundary since the starting temperature was slightly above the critical temperature of ethylene. We notice the small pressure drop in the inlet line, followed by choking at the phase boundary, and then flashing after the choke discontinuity. We note that this flow is choked at the nozzle and the exit of the discharge line.

Also shown in Figure 6 is the vapor quality as a function of piping axial distance. All vapor flow is present in the inlet line, followed by liquid at the choke point, and a twophase mixture in the discharge line. The final exit conditions at the end of the discharge are choked at -32 °C, 17.25 barg, and a mass vapor quality of 37 %.

Figure 6: Pressure profile for relief systems piping with starting ethylene conditions at 100 barg and 10 C

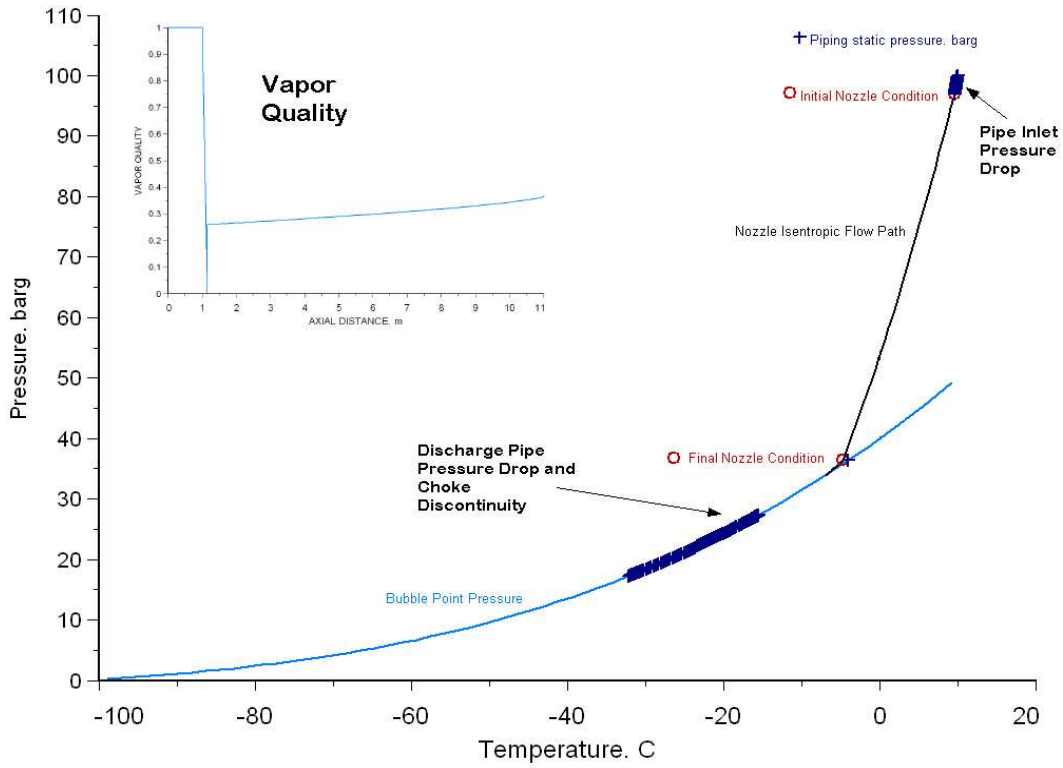

Source: SuperChems Expert

16 Non-equilibrium Nozzle Flow

Current twophase flow methods, such as homogeneous equilibrium flow methods (HEM), can underestimate the flow rate and oversize the relief device, in some instances significantly. The problem is amplified when a larger relief device is installed and the downstream equipment for separation, flaring, and/or vent containment receive much higher flow rates than they were designed for. Oversizing the relief devices can be risky and not knowing the right flow rate can be detrimental to downstream safety systems with a larger device.

Although non-equilibrium flow is well researched, the literature published so far does not provide clear and practical reliable methods for the calculation of non-equilibrium flow for single components or mixtures. We can demonstrate how Equation 4 can also be used for the calculation of non-equilibrium flow.

It has been shown by Fletcher [17, 18] that a length of pipe (or nozzle) of 100 mm ($\simeq$4 inches) is necessary and sufficient to establish equilibrium twophase flow independent of the pipe diameter size. This is also verified by other researchers as shown in Table 3.

Non-equilibrium flow is primarily caused by not having enough residence time to enable nucleation and bubble growth to occur in the flowing liquid. As the pressure drops, and with sufficient residence time, the liquid flashes to vapor and as a result twophase flow occurs where both liquid

Table 3: Required flow distance for equilibrium twophase flow

Author/reference	Diameter (mm)	Length/Diameter	Pipe length (mm)
Fauske [19]	6.35	16	100
Uchida [20]	4	25	100
Ogasawara [21]	10	10	100
Sozzi [22]	12.7	10	127
Van den Akker et al. [23]	4	22	90
Fletcher [17]	3.2	33	105

and vapor flow simultaneously.

For saturated liquids flowing out of nozzles and/or pipes where sufficient residence time is not available to achieve thermodynamic equilibrium, i.e. pipe length which is less than 100 mm, non-equilibrium effects become important in determining the mass flux or mass flow rate. As the available flow length approaches zero, the flow will approach all liquid nozzle or Equation 34 type flow. Equilibrium flow is established at lengths greater than 100 mm.

Figure 7: Freon-11 twophase mass flux as a function of L/D

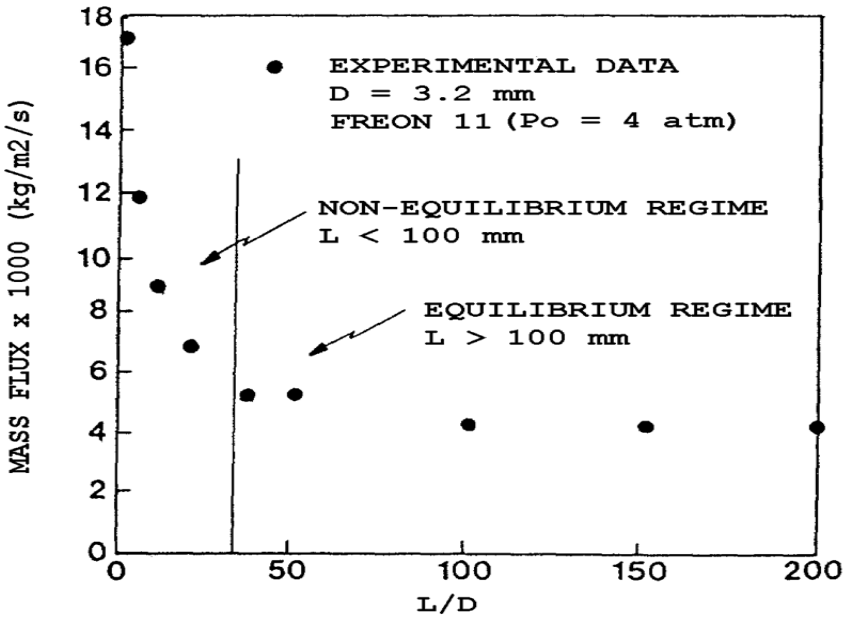

Fauske [24] proposed the following simple equation for estimating twophase mass flux where non-

equilibrium effects are important:

$$G_e = \frac{\lambda}{v_v - v_l}\sqrt{\frac{1}{N c_{p,l} T_o}} \tag{91}$$

where λ is the latent heat of vaporization per unit mass, v is the specific volume, $c_{p,l}$ is the liquid specific heat, T_o is the initial or starting temperature, and N is a non-equilibrium parameter given by:

$$N = 10L + \frac{\lambda^2}{2\Delta P C_d^2 T_o c_{p,l}(v_v - v_l)^2 \rho_l} \tag{92}$$

where L is the pipe length in meters and ΔP is the total available pressure drop in Pascals. Figure 7 shows excellent agreement between Equation 91 and experimental data involving Freon-11.

Equation 91 will reduce to Equation 34 type flow at L = 0. Fauske [24] also approximates twophase flow for subcooled storage conditions by assuming that the choked exit pressure is equal to the saturation pressure at the storage temperature using an Equation 34 flow type equation:

$$G_e = \sqrt{2\rho_{o,l}\left[P_o - P_{o,sat}\right]} \tag{93}$$

Equation 91 reduces to the equilibrium expression for L = 0.1 m. Fauske [24] reports the following equation for estimating homogeneous equilibrium twophase mass flux:

$$G_e = \frac{\lambda}{v_v - v_l}\sqrt{\frac{1}{c_{p,l} T_o}} \tag{94}$$

We use a simple case of ammonia flow to compare the various predictions of Fauske's equations for twophase mass flux described above. The liquid density of ammonia at 297.15 K is 603 $\mathrm{kg/m^3}$, the saturation pressure is 970000 Pa, the latent heat of vaporization is 19900000 J/kmol/K, the liquid heat capacity is 82100 J/kmol/K.

Using the ideal gas law we calculate the vapor density of ammonia at the storage conditions:

$$\rho_v = \frac{P_{sat} M_w}{R_g T_0} = \frac{(9.7 \times 10^5)(17)}{(8314)(297.15)} = 6.67 \ \mathrm{kg/m^3} \tag{95}$$

The saturated storage homogeneous twophase mass flux is calculated using Equation 94 using a discharge coefficient of 1:

$$G_e = \frac{1.99 \times 10^7}{17\left[1/6.67 - 1/603\right]}\sqrt{\frac{17}{(82100)(297.15)}} = 6590 \ \mathrm{kg/m^2/s} \tag{96}$$

For subcooled storage using a pressure of 1.1 saturation value, Equation 93 is used to estimate the mass flux using a discharge coefficient of 1:

$$G_e = \sqrt{2(603)(9.7 \times 10^5)}\sqrt{0.1} = 34202\sqrt{0.1} = 10815 \text{ kg/m}^2/\text{s} \quad (97)$$

At 1.05 times the saturation value, the mass flux is:

$$G_e = 34202\sqrt{0.05} = 7647 \text{ kg/m}^2/\text{s} \quad (98)$$

Darby [25] proposed an adjustment to the vapor quality as a function of nozzle flow length:

$$x = x_o + (x_e - x_o)\frac{L}{L_{\text{equilibrium}}} \quad (99)$$

where x is the local vapor quality adjusted for non-equilibrium, x_o is the initial quality entering the nozzle, x_e is the local vapor quality assuming thermodynamic equilibrium, L is the nozzle length, and $L_{\text{equilibrium}}$ is the nozzle flow length required to achieve equilibrium, typically 100 mm.

Diener and Schmidt [26] (also see ISO 4126-10 [9]) proposed the use of a boiling delay factor N to account for the effects of non-equilibrium:

$$\frac{dx}{dP} = N\frac{dx_e}{dP} \text{ where } N \simeq [x_e(P_{crit})]^a \quad (100)$$

Where N tends to a value of 1 at equilibrium and tends to 0 for non-flashing (frozen) flow. The parameter a is an empirical constant with a value that is less 1. Numerous other methods [27] have also appeared in the literature where the boiling delay factor was incorporated into the omega method as well as other nozzle flow calculations methods. These methods are all empirical in nature and at best semi-empirical.

Burnell's method remains the preferred method because of its fundamental underpinnings and its applicability to mixture as well as pure components.

17 Case Studies for Non-Equilibrium Flow

We provide several practical examples using SuperChems Expert illustrating visually how and why non-equilibrium and RPC flows occur. ioMosaic's SuperChems Expert software is used to model multicomponent non-equilibrium flow and to illustrate how mixture composition influences non-equilibrium flow rates. SuperChems Expert includes detailed steady state and dynamic implementations of nozzle (see Equations 4 and 33) and pipe flow methods.

We illustrate important non-equilibrium concepts using a mixture of C2 (ethane, 30 % by weight) and C7 (heptane, 70 % by weight). A subcooled liquid mixture of C2/C7 flows through an ideal nozzle from a reservoir with stagnation conditions of 40 C and 60 barg. If flow occurs such that

Figure 8: Initially subcooled C2/C7 flow

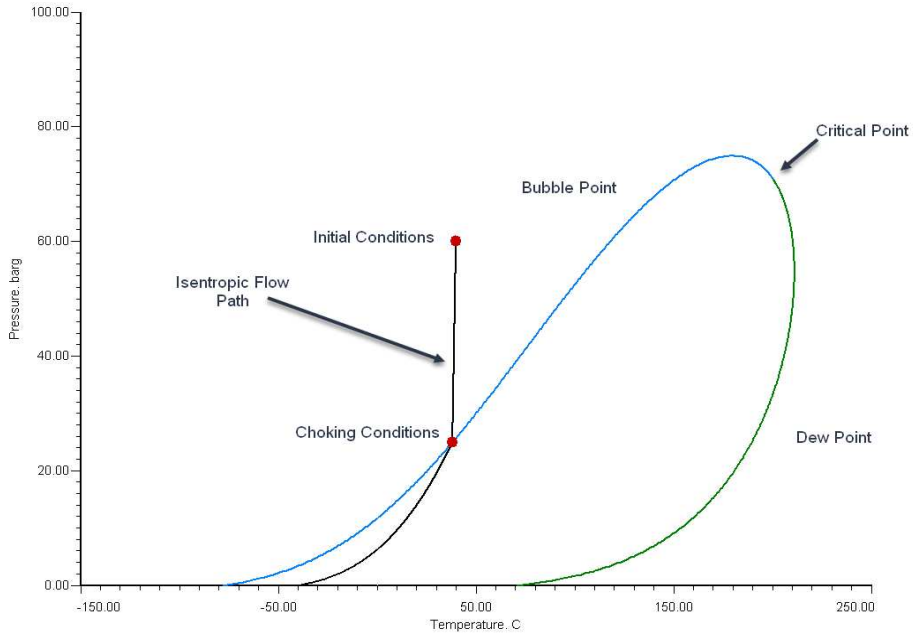

Source: SuperChems Expert

thermal and mechanical equilibrium conditions are achieved, i.e. where there is enough time for flashing to take place, choking conditions will occur at the phase boundary as shown in Figure 8.

As a result, the liquid mass flux can be accurately calculated using an Equation 34 type flow:

$$G_e = \sqrt{2\rho_o \left(P_o - P_{\text{sat}} + \rho_o^2 u_o^2\right)} \tag{101}$$

where P_o is the initial stagnation pressure, T_o is the initial stagnation temperature, and P_{sat} is the bubble point pressure or saturation pressure at the isentropic flow temperature T_b. We note that for liquids, the value of T_b will be approximately equal to T_o, even where the pressure difference between P_o and P_{sat} is large.

The mass flux is calculated for ideal nozzle flow by selecting isentropic end conditions (pressure, temperature, and quality) that maximize flow. This is illustrated graphically in Figure 9. We note the clear change in slope of the mass flux vs. backpressure curve associated with the choke conditions at the phase boundary.

If non-equilibrium effects dominate, i.e. the flow does not have enough time for flashing to occur, the choke point can occur at a lower pressure than the bubble point pressure. This occurs inside the twophase boundary but without flashing. In extreme conditions of non-equilibrium (where the rate of pressure drop is very high), this pressure can reach the thermodynamic stability limit at which spontaneous generation of vapor has to occur regardless of whether there is enough time for bubbles to form or not.

Figure 9: Initially subcooled C2/C7 flow mass flux vs. backpressure

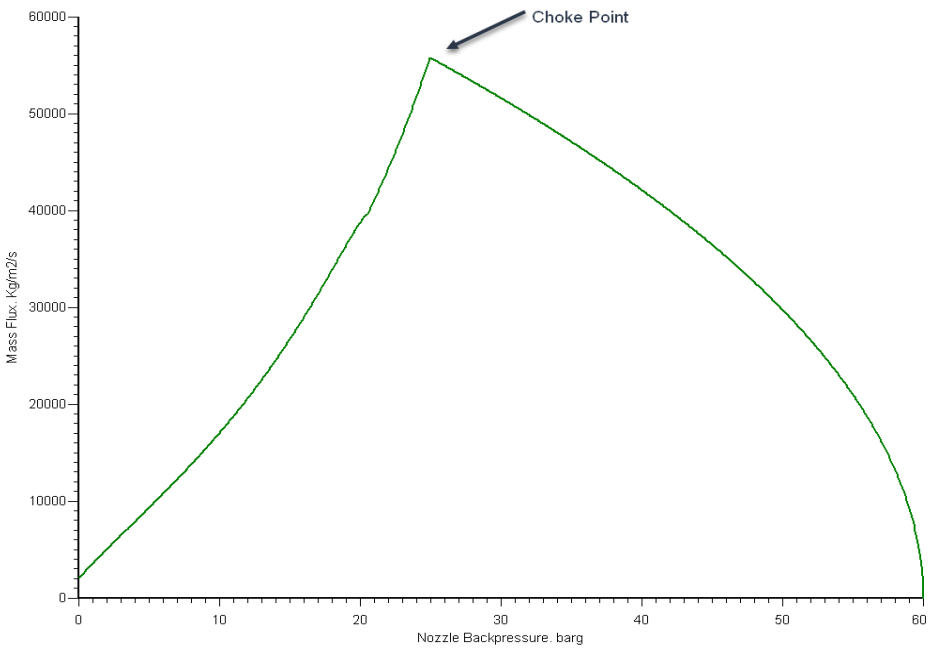

Source: SuperChems Expert

The Equation 34 type flow driving pressure in this case becomes larger and more flow is realized. Non-equilibrium flow becomes less important as the initial temperature gets closer to the critical point. The thermodynamic stability pressure limit is equal to the critical pressure at the critical point. The maximum possible driving pressure for Equation 34 type flow gets smaller as the initial subcooled liquid temperature gets closer to the critical temperature.

Burnell [28] used a bubble delay factor, C, to approximate the impact of non-equilibrium on mass flux by modifying the standard Equation 34 type flow equation:

$$G_e = \sqrt{2\rho_o \left[P_o - (1-C)\, P_{\text{sat}}\right] + \rho_o^2 u_o^2} \tag{102}$$

where C is directly related to the bubble growth delay time and typically ranges from 0.2 to 0.3. The magnitude of C determines the pressure undershoot at the choke point/exit due to the superheating of the liquid. C tends to 0 as the starting initial temperature approaches the critical temperature. Depending on the flow conditions, C can also depend on the length of pipe and initial vapor quality. For pipe flow, it has long been recognized that a pipe flow length of approximately 4 inches [18] is required for equilibrium twophase flow to develop, $C = 0$. Non-equilibrium is most important for nozzle flow (pressure relief valve flow) and for short piping. The above equation can be corrected to reflect the impact of friction on nozzle flow:

$$G_e = \sqrt{\frac{2\rho_o \left[P_o - (1-C)\, P_{\text{sat}}\right] + \rho_o^2 u_o^2}{1 + 4f\frac{l}{d}}} \tag{103}$$

where f is the Fanning friction factor and l/d is the length to diameter ratio of the nozzle and/or

piping. More information about non-equilibrium flow and retrograde and phase change flow can be found in references [11, 8].

If we use a non-equilibrium correction factor of $C = 0.27$ for the C2/C7 example and allow non-equilibrium effects for the ideal nozzle mass flux calculation, we obtain the results shown in Figure 10. Figure 10 also shows an all liquid solution starting at -80 C, an all vapor solution starting at 250 C, and a twophase solution starting at 160 C and 21 % vapor mass fraction in order to contrast and compare typical shapes of mass flux vs. backpressure for liquid, vapor, twophase, and subcooled liquid flows. For all vapor and twophase flashing flow, the correct values of choke pressure and choke temperature are strongly dependent on the numerical accuracy of the calculations and vapor quality. Small deviations in mass flux at the maximum point can lead to large deviations in choke pressure.

The isentropic flow path is shown in Figure 11 along with the thermodynamic stability limit. The calculation of thermodynamic stability limits for vapor and liquid is complex for mixtures and requires an equation of state. In the case of a pure component, an equation of state is still required. However, the thermodynamic stability limit can be approximated with reasonable accuracy as shown in Figure 12. For a pure component, the stability limit temperature at atmospheric pressure is approximately equal to:

$$T_{sl} \simeq 0.92\, T_c \tag{104}$$

where T_c is the critical temperature in Kelvins. If the stagnation temperature T_o of a subcooled liquid pure component is greater or equal to T_{sl} then the choke pressure P_{sat} must be greater or equal to P_{sl}:

$$P_{\text{sat}} \geq P_{sl} \geq P_{atm} + (P_c - P_{atm}) \left[\frac{\frac{T}{T_c} - 0.92}{0.08} \right] \quad \text{where} \quad T_{sl} \leq T \leq T_c \tag{105}$$

Typical Values of C

Numerous publications report values of C for water flow. Reference [29] recommends a value of C as a function of water saturation pressure as shown in Figure 13. The value of C decreases as the the saturation pressure of water increases, i.e. at higher initial stagnation temperatures for the subcooled liquid water. The entire data set is well below the thermodynamic stability limit shown in Figure 12.

More recently, reference [30] recommended similar values for C for water as a function of a dimensionless subcooled temperature number as shown in Table 4.

Sallet [31] correlated C for water with surface tension as a function of temperature as originally suggested by Burnell [28]. Burnell considered a vapor bubble of radius r at the throat of the nozzle ($P = P_{\text{sat}}$) where the pressure is $P_{sat}(T_o)$ inside the bubble because the flow is so rapid that the liquid is still at T_o when the liquid reached the throat:

$$P_{sat}(T_o) - P_{\text{sat}} = \frac{2\sigma}{r} \tag{106}$$

Figure 10: Initially subcooled C2/C7 flow mass flux vs. backpressure, $C = 0.27$

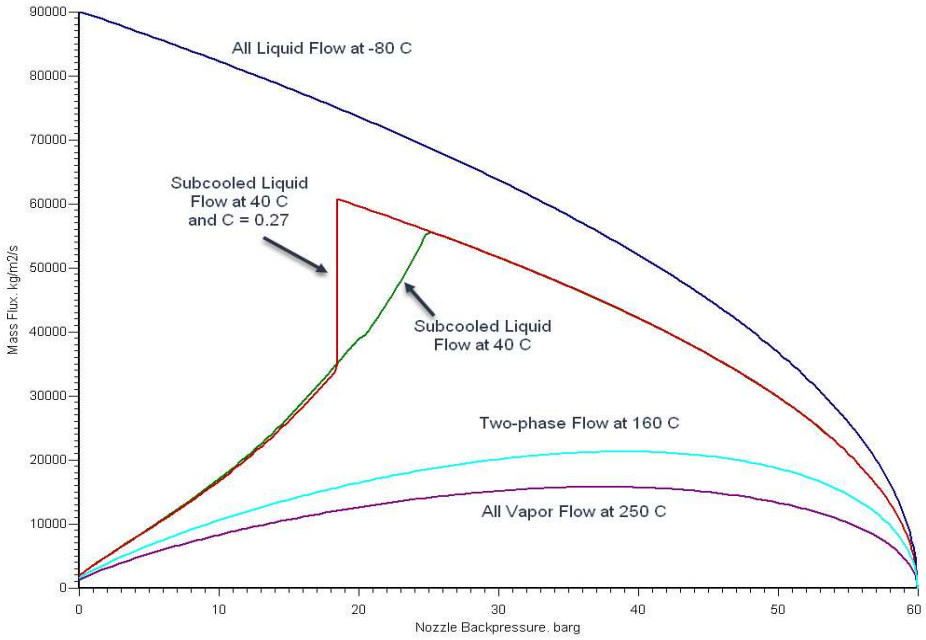

Source: SuperChems Expert

or

$$C = 1 - \frac{P_{\text{sat}}}{P_{sat}(T_o)} = \frac{2\sigma}{rP_{sat}(T_o)} \tag{107}$$

where σ is the surface tension of water. Burnell [28] notes that the product $rP_{sat}(T_o)$ is constant over a large pressure range. As a result, if an actual value of C exists for water at one temperature, one can estimate the C value at a different temperature by using the ratio of the surface tension at those different temperatures:

$$C_o = C_{ref}\frac{\sigma(T_o)}{\sigma(T_{ref})} \tag{108}$$

In theory, we should be able to apply this equation to any fluid where one C value is measured and where surface tension data is available as a function of temperature.

Chemical and mixture specific values of C can be estimated using the modified Lienhard correlation discussed in Melhem [32].

18 Understanding Burnell's C Parameter

Rapid depressuring of a vessel containing saturated liquid can lead to non-equilibrium flow followed by explosive boiling of the liquid contents. Depressuring can be attributed to flow and/or

Figure 11: Initially subcooled C2/C7 flow using $C = 0.27$

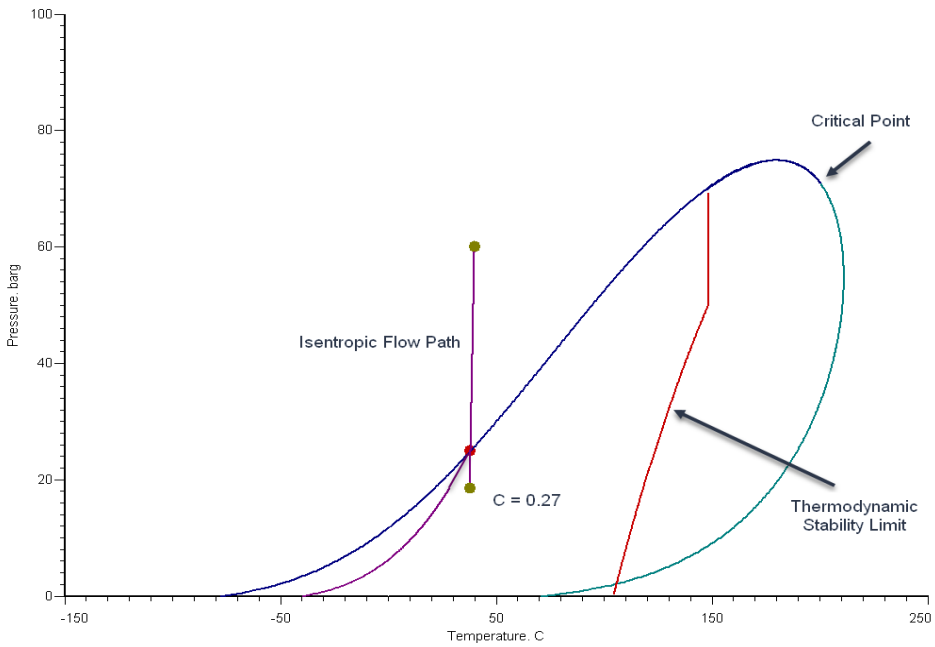

Source: SuperChems Expert

expansion. The same phenomenon, i.e. explosive boiling of liquids, can be induced by rapid heating of the liquid and is sometimes referred to as a rapid phase transition.

As shown to the right for vessel depressuring, the pressure can drop below the saturation point following rapid depressuring. The rate of pressure drop, Σ, influences this pressure undershoot which in turn influences the superheat available for bubble nucleation and growth. A large depressuring rate can lead to a large undershoot and thus a large bubble nucleation and growth superheat.

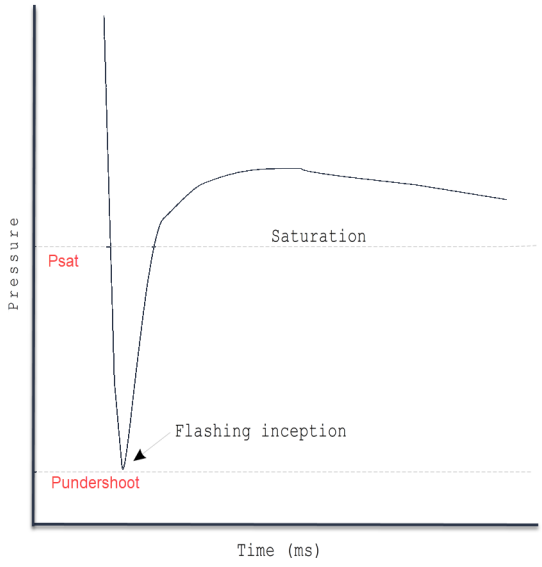

The pressure will recover when the pressure rise caused by bubble generation is equal to the rate of imposed pressure drop at flashing inception. If the rate of pressure drop is large enough, a metastable liquid can form upon depressuring.

A sharp pressure rise caused by homogeneous (spontaneous) and/or heterogeneous bubble generation follows [33, 34, 35, 36]. Heterogeneous nucleation occurs more frequently in flashing flow than homogeneous nucleation. Heterogeneous nucleation is more likely for dirty fluids with suspended impurities, fluids with dissolved gases, and where vessel and piping walls have rough flow surfaces leading to imperfect wetting. Virtually all liquids contain some dissolved gases. The pres-

Figure 12: Thermodynamic stability limit for water

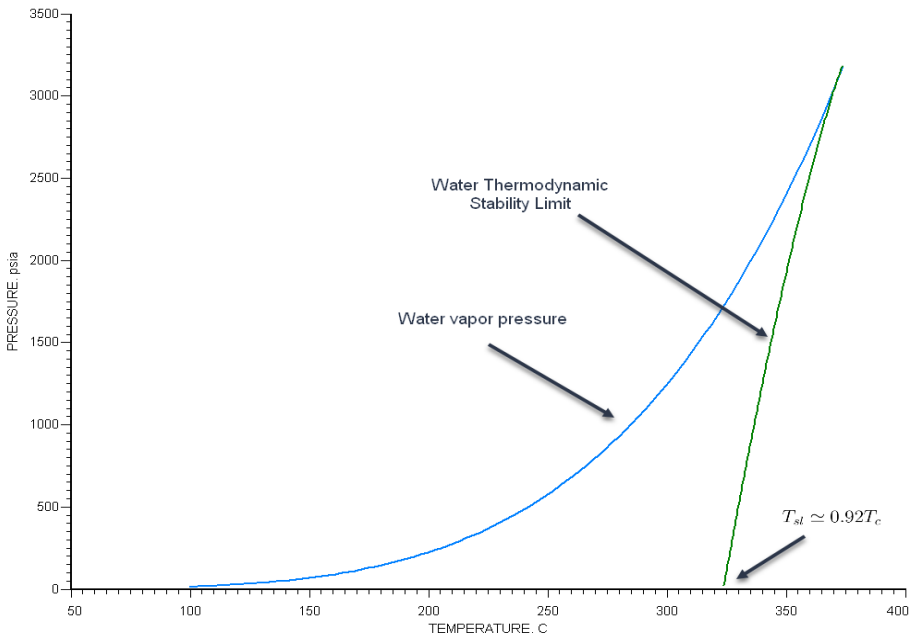

Source: SuperChems Expert

ence of dissolved gas cause the pressure in the bubble to increase totaling the partial pressure of the gas and saturation pressure of the vapor. As a result, the bubble can grow at liquid pressures greater than the vapor pressure.

One should note that rapid depressuring or rapid heating/cooling can render heterogeneous bubble nucleation sites inactive. As the initial temperature/pressure approach critical conditions, depressuring rates required to cause a metastable liquid to form become smaller. Figure 14 illustrates how the flashing process for water can be influenced by rapid pressure drop or rapid heating leading to heterogeneous and/or homogeneous bubble nucleation and growth.

Under a near isothermal pressure drop such as is experienced typically during an isentropic expansion of a subcooled liquid (see path A to B in Figure 14), the pressure drops below the saturation pressure, and at $\Sigma = 0.01$ Matm/s, flashing will occur at a pressure below but near the saturation pressure. At $\Sigma = 1.8$ Matm/s, flashing will occur at a pressure below saturation but near the thermodynamic stability limit. At extremely large values of Σ, flashing will have to occur at the thermodynamic stability limit. Lower values of the undershoot pressure drive more flow for subcooled liquids which is why non-equilibrium liquid flow occurs and is important for pressure relief and vent containment design and evaluation (also see [37]).

The pressure undershoot for water can be estimated from a correlation developed by Lienhard [38,

Figure 13: Recommended Burnell C value for water [29]

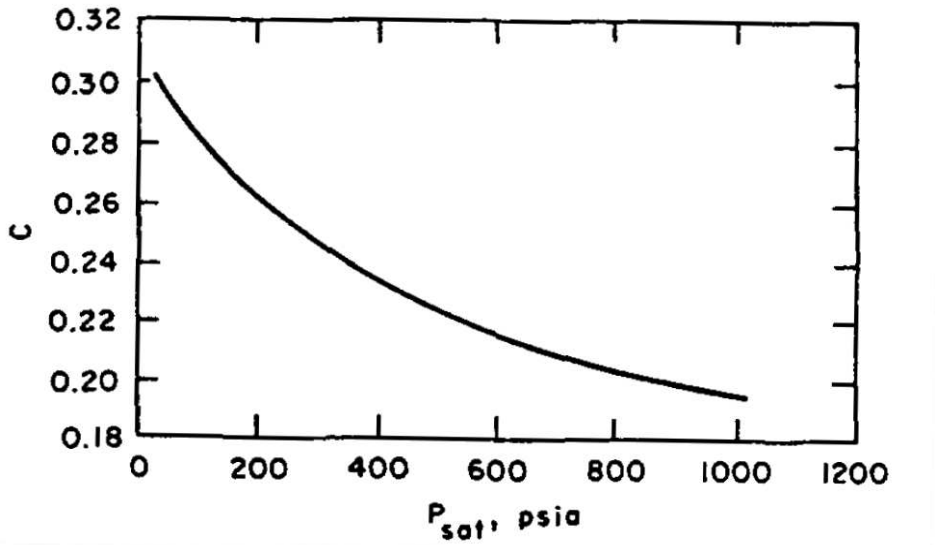

39]:

$$\psi = 0.1058\left[1+14\Sigma^{0.8}\right]\left(\frac{T}{T_c}\right)^{28.46} \tag{109}$$

$$G_b = \frac{W_{cr}}{k_BT} = \frac{16\pi\sigma^3\psi}{3k_BT\left[1-\frac{\rho_{g,sat}}{\rho_{l,sat}}\right]^2\left[P_{\text{sat}}-P_{\text{undershoot}}\right]^2} = 28.2 \tag{110}$$

$$\begin{aligned}\Delta P &= P_{\text{sat}} - P_{\text{undershoot}} \\ &= \underbrace{\left(\sqrt{\frac{0.1058\times 16\pi}{3\times 28.2}}\right)}_{0.250}\left(\frac{\sigma^{3/2}}{\sqrt{k_BT_c}}\right)\left(\frac{\left(\frac{T}{T_c}\right)^{13.73}\left[1+14\Sigma^{0.8}\right]^{1/2}}{\left[1-\frac{\rho_{g,sat}}{\rho_{l,sat}}\right]}\right)\end{aligned} \tag{111}$$

where ψ is Lienhard's heterogeneity factor regressed from measured data, W_{cr} is the net work required to form a bubble having a critical size from classic homogeneous bubble nucleation theory, k_BT is the kinetic energy of the molecules, G_b is the Gibbs number, ΔP is in Pa, T is the initial temperature in Kelvin, $k_B = 1.380649\times10^{-23}$ $\mathrm{J/K}$ is Boltzmann's constant, σ is the liquid surface tension at T in $\mathrm{N/m}$, Σ is the rate of pressure drop in $\mathrm{Matm/s}$ (Mega atmosphere/second), $\rho_{g,sat}$ and $\rho_{l,sat}$ are the mass density of vapor and liquid at equilibrium in $\mathrm{kg/m^3}$, and T_c is the critical temperature in Kelvin. The correlation was developed for:

$$0.62 \leq \frac{T}{T_c} \leq 0.935 \tag{112}$$

$$0.005 \leq \Sigma \leq 1.8 \tag{113}$$

Equation 111 should not be used for lower depressuring rates without changing the equation constants. The rate of pressure drop can include both the contributions of transient vessel blowdown

Table 4: Recommended C values for water [30]

Upstream state	Condition	P_0 (MPa)	C_f	Remark
Subcooled and saturated water	$0.0 \leq \Delta T^*_{sub} < 0.15$	0.5	0.87	10% error
		1.0	0.85	
		2.0, 3.0	0.83	
		4.0–6.0	0.82	
		7.0–20.0	0.81	
	$0.15 \leq \Delta T^*_{sub} \leq 1.0$	0.5–20.0	1.0	5% error
Two-phase mixture	$0.0 < x \leq 1.0$	0.5	0.81	10% error
		1.0	0.80	
		2.0–11.0	0.79	
		12.0, 13.0	0.78	
		14.0–17.0	0.77	
		18.0	0.76	
		19.0, 20.0	0.75	

$C_f = 1 - C$
$\Delta T^*_{sub} = \frac{T_{sat}(P_o) - T_o}{T_{sat}(P_o) - 20}$ where T is in degrees C, P_o is the stagnation pressure, and T_o is the stagnation temperature.

and flow acceleration leading to additional pressure drop in nozzles and/or piping [41]:

$$\Sigma = \underbrace{\left[\frac{\partial P}{\partial t}\right]_z}_{\text{Vessel}} + \underbrace{u\left[\frac{\partial P}{\partial z}\right]_t}_{\text{Nozzle and/or Piping}} \tag{114}$$

$$\underbrace{u\left[\frac{\partial P}{\partial z}\right]_t}_{\text{Nozzle}} \simeq \frac{\dot{m}^3}{\rho^2 A_{\text{noz}}^4}\frac{dA_{\text{noz}}}{dz} = \frac{G^3}{\rho^2}\frac{d\left[\ln A_{\text{noz}}\right]}{dz} \tag{115}$$

where P is the static pressure, z is the flow path length or axial distance, t is time, u is the flow velocity, A_{noz} is the nozzle minimum flow area, G is the mass flux, $\dot{m}$ is the mass flow rate, and ρ is the mass density. Note that Σ is in Matm/s. Flashing inception in nozzles or other flow geometries with restrictions causing flow acceleration will always occur at the throat or plane of minimum flow area. Turbulence may also be generated where flashing occurs. Equation 115 can be used based on the maximum value of dA_{noz}/dz for converging nozzles.

For flow through nozzles and/or piping, the undershoot pressure, $P_{\text{undershoot}}$, can be used to approximate Burnell's [28] constant C:

$$C = 1 - \frac{P_{\text{undershoot}}}{P_{\text{sat}}} \tag{116}$$

Figure 14: Flashing inception following a rapid pressure drop for water

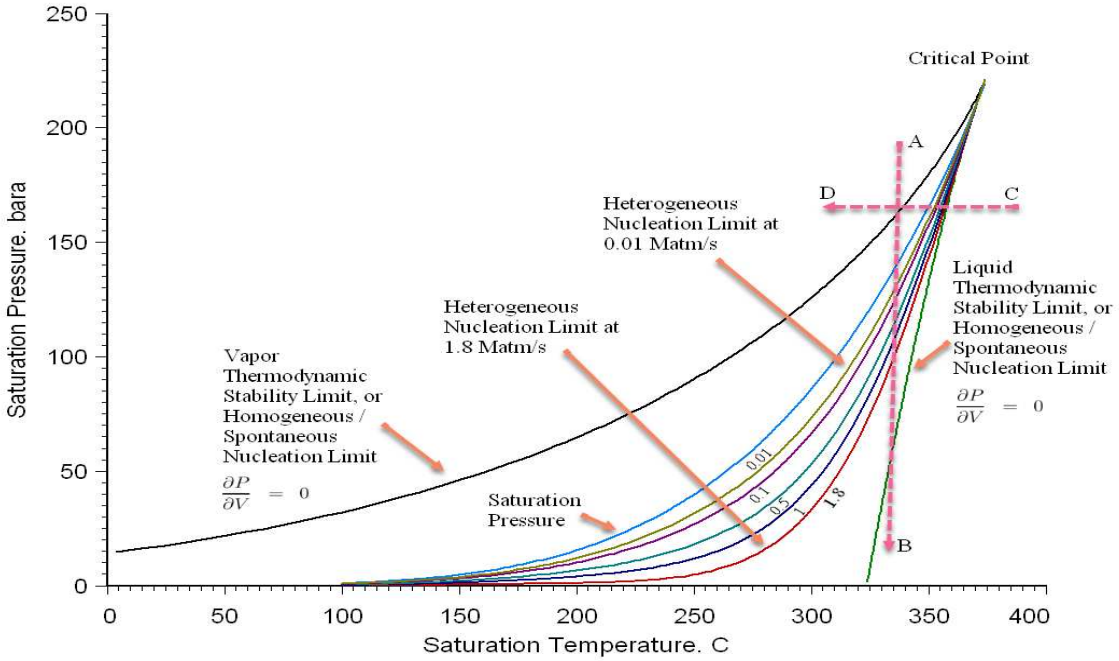

Source: SuperChems Expert

$P_{\text{undershoot}}$ cannot be less than the limit of mechanical/thermodynamic stability often referred to as the homogeneous nucleation limit or superheat limit. For a pure component that limit is established at:

$$\frac{\partial P}{\partial V}\,|_{T,N} \;=\; 0 \tag{117}$$

where V is the fluid volume. For a multicomponent mixture, the limit can still be calculated from an equation of state [14] by setting the determinant of the mixture partial molar chemical potential μ to zero:

$$\det \begin{bmatrix} \frac{\partial \mu_0}{\partial N_0} & \frac{\partial \mu_0}{\partial N_1} & ..... & \frac{\partial \mu_0}{\partial N_{n-1}} \\ ..... & ..... & ..... & ..... \\ ..... & ..... & ..... & ..... \\ \frac{\partial \mu_{n-1}}{\partial N_0} & \frac{\partial \mu_{n-1}}{\partial N_1} & ..... & \frac{\partial \mu_{n-1}}{\partial N_{n-1}} \end{bmatrix} \;=\; 0$$

where N_i is the number of moles of chemical i and n is the total number of chemicals in the mixture.

Concepts pertaining to the thermodynamic stability limits for pure components and mixtures were discussed with emphasis on non-equilibrium and subcooled liquid flows. Both heterogeneous and homogeneous nucleation are thought to be important for non-equilibrium flow. We demonstrated that subcooled liquid flow pressure differential must be bound between $P - P_{\text{sat}}$ and $P - P_{\text{undershoot}}$,

Figure 15: Rapid heating leading to a superheat limit rapid phase transition for an LNG mixture [40]

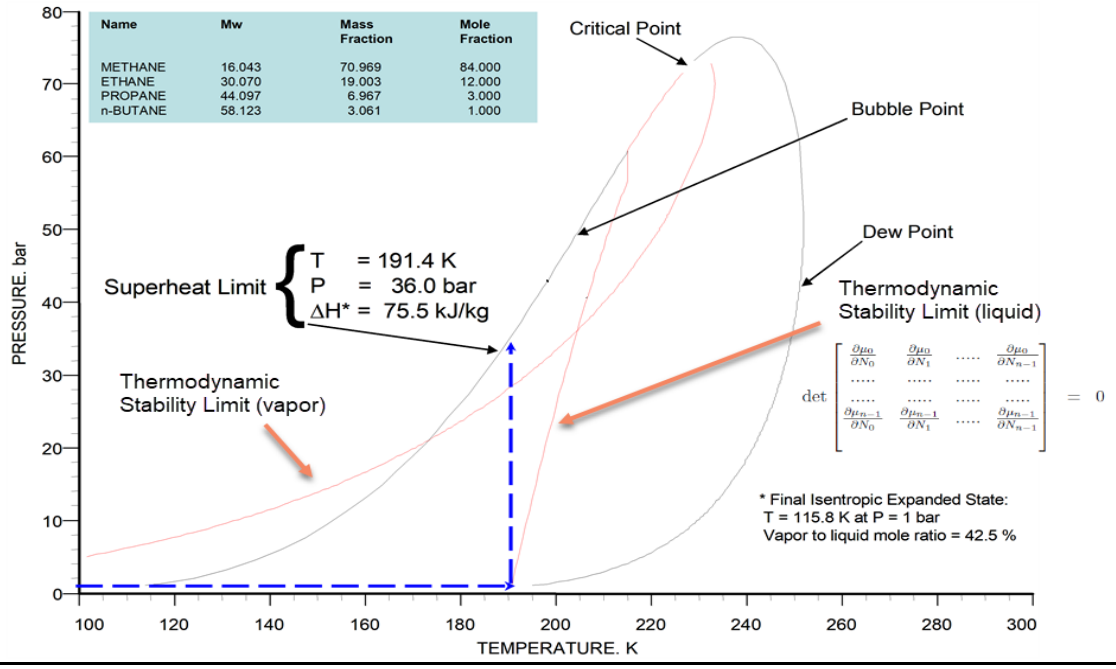

and that $P_{\text{undershoot}}$ cannot be less than the thermodynamic stability limit. The rate of pressure drop Σ required to cause non-equilibrium flow gets smaller as the flow pressure and temperature conditions tend towards the critical point.

19 Generalized Burnell's C Parameter Values

Equation 111 can be extended to other chemicals and mixtures [42, 43] if we assume that Lienhard's heterogeneity correction ψ which depends on reduced temperature applies equally to other chemicals and mixtures. However, the Gibbs number [44], G_b, has to be scaled relative to water:

$$G_b \simeq \underbrace{G_{b,w}}_{28.2} \left[\frac{\sigma}{\sigma_w}\right]^3 \left[\frac{T_{c,w}}{T_c}\right] \left[\frac{P_{\text{sat,w}} - 1}{P_{\text{sat}} - 1}\right]^2 \left[\frac{1 - \frac{\rho_{v,w}}{\rho_{l,w}}}{1 - \frac{\rho_v}{\rho_l}}\right]^2 \tag{118}$$

Where P_{sat} is the saturation or bubble point pressure in bara and ρ is the mass density in kg/m^3 evaluated at a saturation temperature equal to 0.9 times the critical temperature. The surface tension ratio is not very sensitive to temperature and is evaluated at 298.15 K or the normal boiling point. Figure 16 shows a nucleation diagram for Acrylonitrile using Equation 118 yielding $G_b = 49.32$. The scaling proposed in this paper is consistent with the compilation of measured homogeneous nucleation limits for 90 pure substances and 28 mixtures [45].

Figure 16: The superheat and nucleation limits for pure acrylonitrile

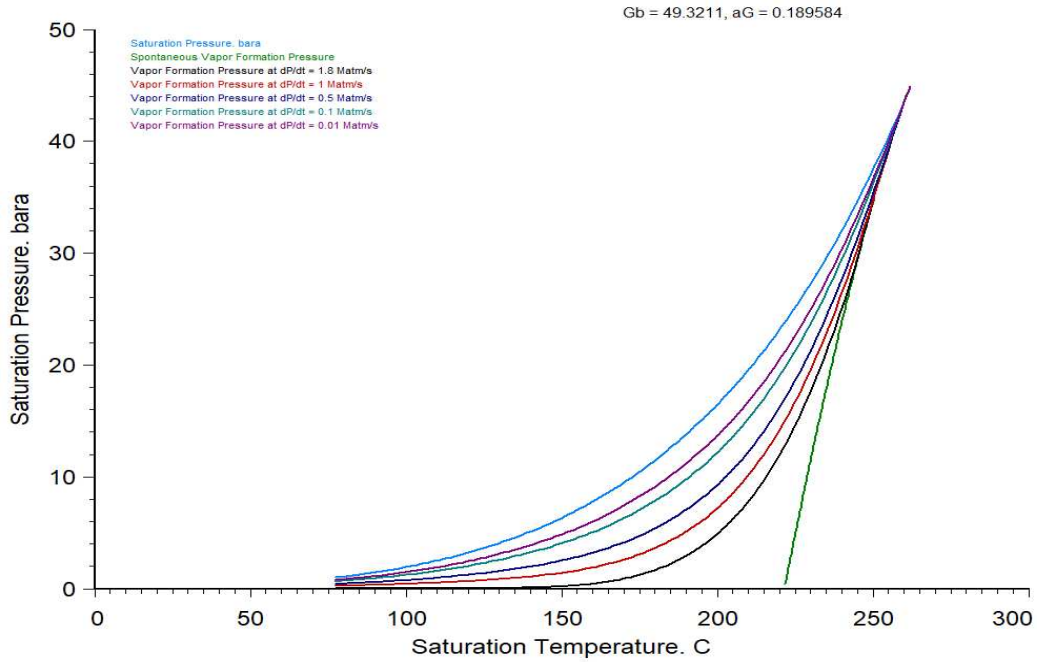

Source: SuperChems Expert

The nucleation limits shown in Figure 16 can be used to calculate Burnell's C constant from Equation 116 at different pressures as shown in Figure 17.

Nucleation limits are shown in Figure 18 for a 50/50 by weight mixture of ethane-butane as calculated by SuperChems Expert . In order for the scaling to work properly for mixtures, the scaling vapor properties must be obtained at the vapor mole fractions in equilibrium with the liquid mole fractions at the bubble point.

20 Guidance for Using SuperChems Expert

Versions 8.20 and higher of SuperChems Expert include options for solving flow applications where RPC flow is possible. The "Set Global Limits" option includes choices for checking the phase boundaries during flow and for the selection of nozzle flow integration methods. This option is most effective in conjunction with the selection of vdP integration for nozzle flow. The option for checking phase boundaries should not be enabled when flow maps are being used for flare systems calculations with the ideal gas behavior option.

The user should always establish a phase envelope or a saturation curve before attempting any flow calculations. Inversion curves can be associated with streams in SuperChems Expert and are very useful for high pressure applications.

Although the SuperChems Expert pipe flow and nozzle flow modules allow the user to specify the starting phase of flow, it is highly recommended to allow the module to determine the starting

Figure 17: Burnell's C constant for pure acrylonitrile

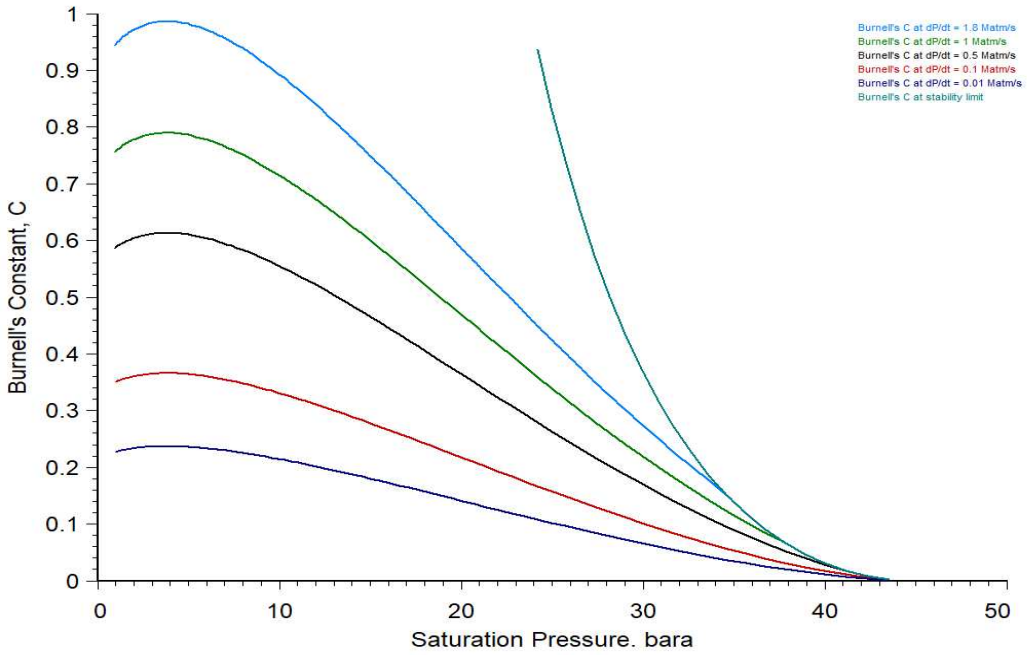

Source: SuperChems Expert

phase by selecting the "Determine Flow Phase" option. Care must be exercised when dealing with pure components where the starting temperature is very close to the saturation point due to small deviations of the vapor pressure equations used. In these cases, a better approach is to specify the pressure and starting vapor fraction and to let the code select the coincident temperature. Use of the ideal nozzle or stream flow options in conjunction with flashing of the choke point (by conserving stagnation enthalpy) to ambient or user imposed back pressure will help the user select the appropriate pipe flow module.

When the phase boundary check options are enabled, the single phase piping and nozzle flow modules will detect phase change and issue an error or warning message to the user recommending the use of the twophase pipe flow module.

21 Conclusions

The omega method can be used for single component flow estimates within the proposed limits by ISO 4126-10 [9]. However, the omega method should not be used for multicomponent systems and/or reaction systems unless the omega parameter is regressed from reliable flash calculations that consider retrograde and phase change at a sufficient number of pressure points. As a result, one has to question the usefulness of the omega method since the generation of multiple flash points can easily be used to develop a numerical vdP integral instead with many less limitations and without introducing additional regression errors.

Direct vdP integration should be the method of choice for nozzle flow because of its wide appli-

Figure 18: The superheat and nucleation limits for a 50/50 by weight mixture of ethane-butane

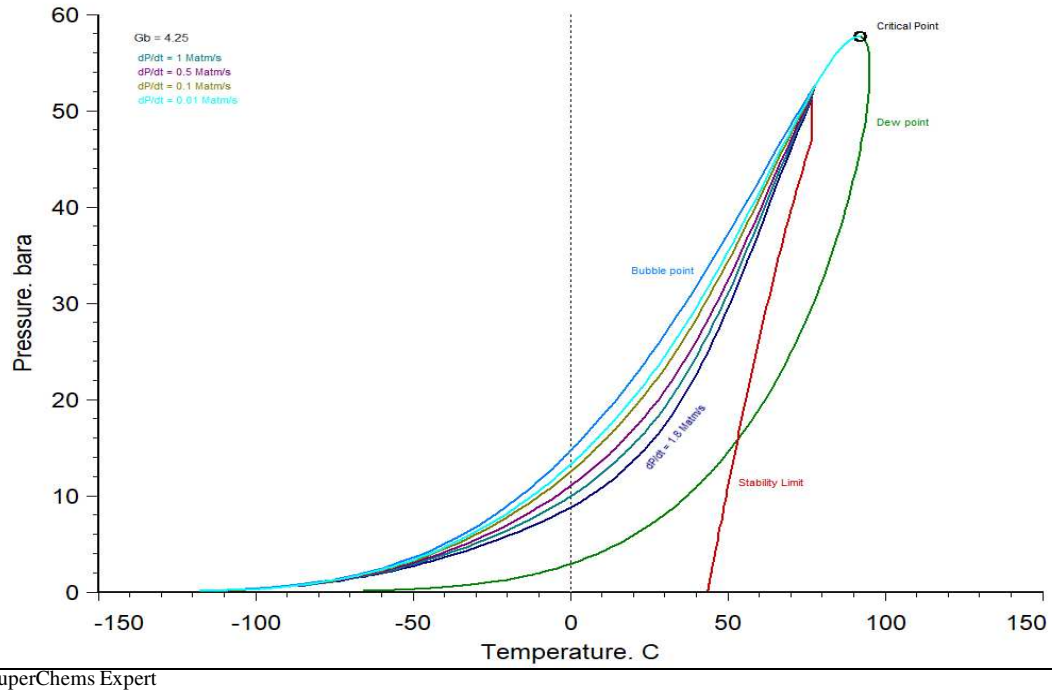

Source: SuperChems Expert

cability and simplicity. The Δh method should be the method of choice for all gas flow without phase change because of its simplicity, accuracy, and speed. Critical to the success of nozzle flow methods is the ability of the software performing the flash calculations to resolve the retrograde and phase change that occurs during the flash calculations. These features are seamlessly integrated in all of the SuperChems Expert robust flow methods.

Non-equilibrium and RPC flow considerations are especially important for emergency relief and flare systems design and evaluations. Improper calculation of non-equilibrium and/or RPC flow rates, especially for subcooled liquid flows near the twophase boundary, can result in significantly undersized or oversized pressure relief devices.

A Useful Definitions

Void Fraction:

This is defined as the ratio of flow cross sectional area occupied by the vapor or gas to the total cross sectional area, $A_T = A_v + A_l$:

$$\alpha = \frac{A_v}{A_T} \tag{119}$$

Slip Velocity:

When dealing with flows involving two phases which differ in density and/or viscosity, the phase that is less dense tends to flow at a higher velocity than the other. The difference between the individual phase velocities is referred to as the slip velocity:

$$u_{vl} = u_v - u_l \tag{120}$$

Slip Ratio:

This is defined as the ratio of the vapor to the liquid velocity and is also referred to as hold-up ratio:

$$u_r = \frac{u_v}{u_l} \tag{121}$$

Superficial Velocity:

For a given phase, this is defined as the velocity of the phase as if it is occupying the entire flow cross sectional area. The liquid superficial velocity is then:

$$u_{sl} = \frac{u_l A_l}{A_T} = u_l \left(1 - \alpha\right) \tag{122}$$

and the vapor superficial velocity is:

$$u_{sv} = \frac{u_v A_v}{A_T} = u_v \alpha \tag{123}$$

Mass Flux:

This is defined as the product of mass and velocity:

$$G = \rho u \tag{124}$$

Isentropic Flash Fraction:

This is also referred to as the isentropic vapor quality which we define as the vapor fraction at the end state following a constant entropy process:

$$x_s = \frac{s_o - s_{e,l}}{s_{e,v} - s_{e,l}} \tag{125}$$

Isenthalpic Flash Fraction:

This is also referred to as the isenthalpic vapor quality which we define as the vapor fraction at the end state following a constant enthalpy process:

$$x_h = \frac{h_o - h_{e,l}}{h_{e,v} - h_{e,l}} \tag{126}$$

Vapor Quality:

This is defined as the ratio of vapor mass flow to total mass flow or vapor mass fraction:

$$x = \frac{G_v A_v}{G_v A_v + G_l A_l} = \frac{1}{1 + \left[\frac{\rho_l u_l (1-\alpha)}{\rho_v u_v \alpha}\right]} \tag{127}$$

References

[1] G. A. Melhem. Retrograde and phase change (RPC) flow considerations for relief and flare systems. *ioMosaic Corporation White Paper*, 2018.

[2] G. A. Melhem. Retrograde and phase change (RPC) flow considerations for relief and depressuring systems. *ioMosaic Corporation White Paper*, 2018.

[3] J. Leung. Sizing of pressure relief devices and associated piping for multiphase flows. In *2nd International Symposium on Runaway reactions, Pressure Relief Design and Effluent Handling, G. A. Melhem and H. G. Fisher, Editors*, pages 319–351. DIERS, AIChE, 1998.

[4] J. C. Leung. Easily size relief devices and piping for two-phase flow. *Chemical Engineering Progress*, 92(12):28–49, 1996.

[5] L. L. Simpson. Fire exposure of liquid-filled vessels. *Process Safety Progress*, 20(1):27–32, 2002.

[6] G. A. Melhem and H. G. Fisher. An overview of SuperChems for DIERS: A program for emergency relief system and effluent handling designs. *Process Safety Progress*, 16(3), 1997.

[7] G. A. Melhem, H. G. Fisher, and D. A. Shaw. An advanced method for the estimation of reaction kinetics, scale-up, and pressure relief design. *Process Safety Progress*, 1994.

[8] G. A. Melhem. On the selection of two-phase flow methods for ERS design. In *European DIERS Users Group Meeting, Lyon, France*. EDUG, 2005.

[9] The International Organization for Standardization. Safety devices for protection against excessive pressure - Part 10: Sizing of safety valves for gas/liquid two-phase flow, 2010.

[10] A. Guinea and J. Basco. Complex versus simplified pressure relief valves sizing methods for two-phase flow. In *DIERS EDUG Meeting, Tarragona, Spain*. EDUG, June 2016.

[11] G. A. Melhem. SuperChems ideal nozzle flow models enhancements - supercritical and subcooled flow. In *DIERS Users Group Meeting, Las Vegas*, 2008.

[12] G. A. Melhem. DIERS technology fundamentals Part III - Two phase flow methods. In *DIERS Fall Virtual Meeting*. AIChE, August 2020.

[13] L. L. Simpson. Navigating the two phase maze. In *International Symposium on Runaway reactions and Pressure Relief, G. A. Melhem and H. G. Fisher, Editors*, pages 394–415. DIERS, AIChE, 1995.

[14] G. A. Melhem, R. Saini, and B. M. Goodwin. A modified Peng-Robinson equation of state. *Fluid Phase Equilibria*, 47:189–237, 1989.

[15] G. A. Melhem, R. Saini, and C. F. Leibovici. On the application of concentration dependent mixing rules to systems containing large numbers of compounds. In *2nd International Symposium of SuperCritical Fluids*, pages 475–477, May 1991.

[16] G. A. Melhem. A general purpose method for the estimation of multiple chokes in gas-vapor and two-phase flow. In *DIERS Users Group Meeting*. AIChE, October 1997.

[17] B. Fletcher and A. E. Johnson. The discharge of superheated liquids from pipes. *I. Chem. E. Symposium Series*, 85, 1984.

[18] B. Fletcher. Flashing through orifices and pipes. AIChE Loss Prevention Symposium in Denver, 1983.

[19] H. K. Fauske. The discharge of saturated water through tubes. *Chemical Engineering Progress Symposium Series*, 61:210–216, 1965.

[20] H. Uchida and H. Nariari. Discharge of saturated water through pipes and orifices. In *3rd International Heat Transfer Conference*. American Institute of Chemical Engineers, AIChE, 1966.

[21] H. Ogasawara. *Bull JSME*, 12(52):837–846, 1969.

[22] G. L. Sozzi and W. A. Sutherland. Critical flow of saturated and subcooled water at high pressure. In *Non-equilibrium two-phase flows*. ASHE winter annual meeting, ASHE, 1975.

[23] H. E. A. Van Den Akker, H. Snoey, and H. Spoelstra. Discharges of pressurized liquified gases through appertures and pipes. In *4th International Symposium on Loss Prevention and Safety Promotion in the Process Industries*, 1983.

[24] H. K. Fauske. Flashing flow: Some practical guidelines for emergency releases. *Plant/Operations Progress*, 4(3):132, 1985.

[25] R. Darby. On two-phase frozen and flashing flows in safety relief values. recommended calculation method and the proper use of the discharge coefficient. *Journal of Loss Prevention*, 17:255–259, April 2004.

[26] R. Diener and J. Schmidt. Sizing of throttling device for gas/liquid two-phase flow part 1: Safety valves. *Process Safety Progress*, 23(4):335–344, December 2004.

[27] J. Leung. A non-equilibrium flow model for initially saturated and subcooled liquid discharge. In *DIERS EDUG Meeting, Hamburg, Germany*. EDUG, June 2011.

[28] J. G. Burnell. Flow of boiling water through nozzles, orifices, and pipes. *Engineering Lond.*, 164:572, 1947.

[29] J. Weisman and A. Tentner. Models for estimation of critical flow in two-phase systems. *Progress in Nuclear Energy*, 2:183–197, 1978.

[30] Yeon-Sik Kim. A proposed correlation for critical flow rate of water flow. *Nuclear Engineering Technology*, 47:135–138, 2015.

[31] D. Sallet and G. Somers. Flow capacity and response of safety relief valves to saturated water flow. *Plant/Operations Progress*, 4(4):207–216, 1985.

[32] G. A. Melhem. Quantify non-equilibrium flow and rapid phase transitions (RPT). *ioMosaic Corporation White Paper*, 2020.

[33] G. A. Melhem, P. A. Croce, and H. Abraham. Data summary and analysis of NFPA's BLEVE tests. *Process Safety Progress*, 12(2):76–82, 1993.

[34] CSB. Williams Geismar olefins plant reboiler rupture and fire, Geismar, Louisiana. Technical Report 2013-03-I-LA, U.S. Chemical Safety and Hazard Investigation Board, 2013.

[35] G. A. Melhem. Catastrophic vessel failure due to thermal expansion of liquids: Williams geismar case study. In *DIERS Users Group Meeting, Houston*. DIERS, AIChE, April 2017.

[36] G. A. Melhem. Thermal expansion relief requirements for liquids, vapors, and supercritical fluids. *ioMosaic Corporation White Paper*, 2018.

[37] G. Hendrickson, G. A. Melhem, R. D'Alessandro, H. Fisher, M. Levin, D. Smith, and L. Korelstein. Geometric and thermodynamic considerations of saturated and slightly subcooled water flow through nozzles. *Chemical Engineering Science*, 254:1–16, 2022.

[38] J. H. Lienhard, N. Shamsundar, and P. O. Biney. Spinodal lines and equations of state: A review. *Nuclear Engineering and Design*, 95:297–314, 1986.

[39] S. Yin, N. Wang, and H. Wang. Nucleation and flashing inception in flashing flows: A review and model comparison. *International Journal of Heat and Mass Transfer*, 146:1–17, 2020.

[40] G. A. Melhem, H. Ozog, and S. Saraf. Understand LNG rapid phase transitions. *Hydrocarbon Processing*, 85:53–59, 2006.

[41] N. Abuaf, O. C. Jones Jr., and B. J. C. Wu. Critical flashing flows in nozzles with subcooled inlet conditions. *Journal of Heat Transfer*, 105:379–383, 1983.

[42] C. F. Delale. The classical theory of homogeneous bubble nucleation revisited. In *5th International Symposium on Cavitation*. Osaka, Japan, November 2003.

[43] J. Lienhard, N. Shamsundar, and P. Biney. Spinodal lines and equations of state: A review. *Nuclear Engineering and Design*, 95:297–314, 1986.

[44] P. O. Biney, W. Dong, and J. H. Lienhard. Use of a cubic equation of state to predict surface tension and spinodal limits. *Journal of Heat Transfer*, 108:405–410, 1986.

[45] C. T. Avedisian. The homogeneous nucleation limits of liquids. *Journal of Physical and Chemical Reference Data*, 14(3):695–729, 1985.

Index

About the Author

Dr. Melhem is an internationally known pressure relief and flare systems, chemical reaction systems, process safety, and risk analysis expert. In this regard he has provided consulting, design services, expert testimony, incident investigation, and incident reconstruction for a large number of clients. Since 1988, he has conducted and participated in numerous studies focused on the risks associated with process industries fixed facilities, facility siting, business interruption, and transportation.

Prior to founding ioMosaic Corporation, Dr. Melhem was president of Pyxsys Corporation; a technology subsidiary of Arthur D. Little Inc. Prior to Pyxsys and during his twelve years tenure at Arthur D. Little, Dr. Melhem was a vice president of Arthur D. Little and managing director of its Global Safety and Risk Management Practice and Process Safety and Reaction Engineering Laboratories.

Dr. Melhem holds a Ph.D. and an M.S. in Chemical Engineering, as well as a B.S. in Chemical Engineering with a minor in Industrial Engineering, all from Northeastern University. In addition, he has completed executive training in the areas of Finance and Strategic Sales Management at the Harvard Business School. Dr. Melhem is a Fellow of the American Institute of Chemical Engineers (AIChE) and Vice Chair of the AIChE Design Institute for Emergency Relief Systems (DiERS).

Contact Information

Georges. A. Melhem, Ph.D., FAIChE
E-mail. melhem@iomosaic.com

ioMosaic Corporation
93 Stiles Road
Salem, New Hampshire 03079
Tel. 603.893.7009, x 1001
Fax. 603.251.8384
web. www.iomosaic.com

How can we help?

Please visit www.iomosaic.com and www.iokinetic.com to preview numerous publications on process safety management, chemical reactivity and dust hazards characterization, safety moments, video papers, software solutions, and online training.

In addition to our deep experience in process safety management (PSM) and the conduct of large-scale site wide relief systems evaluations by both static and dynamic methods, we understand the many non-technical and subtle aspects of regulatory compliance and legal requirements. When you work with ioMosaic you have a trusted ISO certified partner that you can rely on for assistance and support with the lifecycle costs of relief systems to achieve optimal risk reduction and PSM compliance that you can evergreen. We invite you to connect the dots with ioMosaic.

We also offer laboratory testing services through ioKinetic for the characterization of chemical reactivity and dust/flammability hazards. ioKinetic is an ISO accredited, ultramodern testing facility that can assist in minimizing operational risks. Our experienced professionals will help you define what you need, conduct the testing, interpret the data, and conduct detailed analysis. All with the goal of helping you identify your hazards, define and control your risk.

ioMosaic®

Minimizing risk. Maximizing potential.®

US Offices

New Hampshire (Salem) – *Headquarters*
Texas (Houston)
Minnesota (Minneapolis)
California (Berkeley)

International Offices

Kingdom of Bahrain (Al Seef)
United Kingdom (Bath)

Software Solutions

Process Safety Enterprise®
Centralize the process safety management lifecycle to accelerate business goals

Process Safety Office®
Identify, evaluate, and control process hazards with tools used by process safety consultants

Process Safety Learning®
Build your process safety competencies incrementally with online training

Process Safety tv®
View, share, and discuss PSM worldwide on a secure platform

Contact Us

www.ioMosaic.com
sales@ioMosaic.com
1.844.ioMosaic

About ioMosaic Corporation

Through innovation and dedication to continual improvement, ioMosaic has become a leading provider of integrated process safety and risk management solutions. ioMosaic has expertise in a wide variety of areas, including pressure relief systems design, process safety management, expert litigation support, laboratory services, training and software development.

As a certified ISO 9001:2015 Quality Management System (QMS) company, ioMosaic offers integrated process safety and risk management services to help you manage and reduce episodic risk. Because when safety, efficiency, and compliance are improved, you can sleep better at night. Our extensive expertise allows us the flexibility, resources, and capabilities to determine what you need to reduce and manage episodic risk, maintain compliance, and prevent injuries and catastrophic incidents.

Our mission is to help you protect your people, plant, stakeholder value, and our planet.

Consulting Services

- Asset Integrity
- Auditing and Due Diligence
- Combustible Dust Hazard Analysis and Testing
- Facility Siting
- Fault Tree/SIL/SIS Analysis
- Fire and Explosion Dynamics
- Incident Investigation, Litigation Support and Expert Testimony
- Liquefied Natural Gas Safety
- Pipeline Safety
- Process Engineering Design and Support
- Process Hazards Analysis (PHA)
- Process Safety Management (PSM)
- Reactive Chemicals Evaluation and Testing
- Relief and Flare Systems Design and Evaluations
- Risk Management Program Development
- Quantitative Risk Assessments (QRA)
- Software Solutions
- Structural Dynamics
- Training

Laboratory Testing Services (ISO accredited)

- Chemical Reactivity
- Combustible Dust
- Battery Safety
- Specialized Testing